Journal of Water Process Engineering 67 (2024) 106180

Contents lists available at ScienceDirect

Journal of Water Process Engineering

journal homepage: www.elsevier.com/locate/jwpe

Nanoclays in water treatment: Core concepts, modifications, and application insights

Luiz Daniel da Silva Neto [a,b,1], Ali Maged [c,d,*,1], Rafaela Gabriel [b], Pollyanna V.S. Lins [b], Nils H. Haneklaus [e,f], Mark W. Hlawitschka [c], Lucas Meili [b]

[a] Drying Center of Pastes, Suspensions, and Seeds, Department of Chemical Engineering, Federal University of São Carlos (UFSCar), São Carlos, São Paulo 13565-905, Brazil
[b] Laboratory of Processes, Center of Technology, Federal University of Alagoas, Av. Lourival Melo Mota, s/n, Campus A.C. Simões, Tabuleiro do Martins, Maceió, AL 57072-970, Brazil
[c] Institute of Process Engineering, Johannes Kepler University Linz, Altenberger Straße 69, 4040 Linz, Austria
[d] Geology Department, Faculty of Science, Suez University, 43221 Suez, Egypt
[e] Td-Lab Sustainable Mineral Resources, Universität für Weiterbildung Krems, Dr. Karl-Dorrek-Straße 30, 3500 Krems an der Donau, Austria
[f] North-West University, Unit for Energy and Technology Systems - Nuclear Engineering, 11 Hoffman Street, Potchefstroom 2520, South Africa

ARTICLE INFO

Keywords:
Nanoclays
Adsorption
Water treatment
Sorption mechanisms
Synthesis processes

ABSTRACT

Water treatment faces significant challenges due to the presence of diverse and persistent pollutants, necessitating the development of effective and eco-friendly materials. Therefore, nanoclays (NCs) have emerged as promising nanomaterials for water treatment applications. The efficacy of various NCs as adsorbents is attributed to their remarkable properties, such as high specific surface areas (up to 950 m^2/g) and significant cation exchange capacities (up to 150 meq/100 g). This review encompasses the synthesis methods, modification techniques, and characterization approaches utilized in the development of NCs adsorbents, with an emphasis on understanding the structural complexity of NCs and their composites. NCs with exfoliated nanosheets demonstrate markedly improved efficacy due to the full exposure of their reactive sites. The NCs role in the simultaneous adsorption of various pollutants is highlighted, showcasing their capacity to effectively remove multiple contaminants from water in a single treatment process. Furthermore, the adsorption mechanisms and efficiency of NCs in removing varied contaminants are explored. Literature findings indicate that 2:1 clay exhibits superior removal capabilities compared to 1:1 clay for a majority of aquatic pollutants. Various techniques, including chemical treatment, thermal, and biological degradation, have been reviewed for the regeneration of spent NCs, demonstrating differing regeneration performance depending on the technique employed. The review also delves into the potential challenges and future outlook of utilizing NCs in water treatment, offering suggestions for further research, thereby emphasizing the crucial role of NCs in addressing water pollution and their promise in developing sustainable water remediation systems.

1. Introduction

Nanotechnology is widely recognized as a potent approach for environmental remediation via the distinctive physical attributes of nanoscale materials. Nanotechnology presents numerous advantages, including reduced environmental footprint, enhanced speed and efficiency, adaptability to diverse environmental conditions, applicability for in situ remediation, and sustained effectiveness over extended periods. These beneficial features underscore the potential of nanotechnology to address environmental challenges effectively and sustainably [1]. Nanoclay (NC) stands out as a successful nanotechnology approach, demonstrating remarkable efficacy in diverse environmental remediation applications. Various NCs have gained popularity in the environmental industry and bioremediation [2]. Typically, NCs have been employed in adsorption to remove various pollutants, including pesticides, heavy metals, dyes, and antibiotics. NC has proven particularly effective in water treatment applications with its unique properties and high surface area [3].

* Corresponding author at: Institute of Process Engineering, JKU Linz, Austria.
E-mail address: Ali.Maged@suezuni.edu.eg (A. Maged).
[1] These authors share co-first authorship.

https://doi.org/10.1016/j.jwpe.2024.106180
Received 6 July 2024; Received in revised form 13 September 2024; Accepted 13 September 2024
Available online 28 September 2024

A large family of natural or artificial clay minerals known as "nanoclays" have at least one dimension in the nano-range order and are characterized by a layered structure [4]. The cohesion between these layers is predominantly governed by electrostatic interactions and van der Waals forces, aligning them parallel to each other. Comprising mainly metal oxides and remnants of organic matter, NCs exhibit varying concentrations of iron, magnesium, alkaline earth metals, alkali metals, and other cations. The arrangement of clay sheets plays a crucial role in defining the distinctive characteristics of NCs. Numerous uses of these NCs in different sectors have been investigated [5–7]. NCs often have high porosity, large surface areas, and small particle sizes. These materials are an excellent choice for various environmental applications since they are affordable, have a remarkable cation exchange capacity (CEC), and unique structure [8].

This review aims to comprehensively discuss the utilization of NCs in water treatment, focusing on their adsorption capabilities for various pollutants. This article reviewed the varied synthesis processes employed to fabricate NCs and their impact on the adsorption efficiency and overall performance in water treatment applications. Moreover, this review also explores the methods used to characterize NC properties, such as specific surface area, cation exchange capacity, and structural morphology. This review discusses the simultaneous adsorption of multiple pollutants using NCs, emphasizing their role in real wastewater treatment and the underlying sorption mechanisms. Table S1 compares the distinguished features of present review with previously published reviews (≤6 years) on role of NCs in water treatment. The comparison showed that this review is the first to integrate varied critical aspects into one article. Most existing reviews focus only on a limited range of topics, as outlined in Table S1, while the present review provides a more holistic view by addressing multiple dimensions of NC adsorbent applications in water treatment. Therefore, the current review aims to fill important gaps that have not been thoroughly covered in previous literature. This review also incorporates information about the sustainability assessment and economic feasibility of NCs, offering insights into their long-term viability and cost-effectiveness compared to conventional adsorbents. These aspects are crucial for understanding the broader implications of using NCs in water treatment applications. Furthermore, the review refers to NC-based water treatment's limitations, challenges, and future directions.

2. Nanoclays

This section provides an overview of NCs, including their general characteristics and classification. It also discusses the most commonly used types in water treatment, i.e., kaolinite, halloysite, laponite, and montmorillonite, highlighting their unique properties and roles in adsorbing pollutants. NC is a common term given to mineral clays with a laminar structure in the order of nanometers (1–100 nm). It is worth noting that only one dimension needs to be nanometric for such classification, and the other dimensions can be micro-sized due to agglomerations or structure, for instance, montmorillonite, which is nano in one dimension and micro in the other [5]. Compared to other nanometric materials with a layered structure, natural NCs stand out for their diversity, large reserves, low cost, rich composition of elements, diverse morphology, crystalline structure, and ion exchange capacity, providing them unique chemical and physical properties [9].

Clay minerals arise from the chemical weathering of silicate rocks. These layered silicates, known as phyllosilicates, boast a crystalline structure with diverse elemental compositions. These layers comprise two principal structural units: tetrahedral (SiO_4) and octahedral (AlO_6) sheets [10]. The general chemical formula of clay minerals is: (Ca, Na, H) (Al, Mg, Fe, Zn)$_2$(Si, Al)$_4O_{10}(OH)_{2-x}H_2O$, where x represents the amount of water [11]. Alterations in environmental conditions, such as moisture levels, can prompt clay to release or absorb water, leading to various clay types. NCs can be of synthetic or natural origin. Natural clays have silicon and oxygen as ordinary elements in all their compositions [11]. When combined with other elements (i.e., Al, Mg, Fe, Ca, and Na), and considering the varied combinations possible, they yield numerous potential arrangements. One notable trait of clay minerals is their capacity to alter in volume through the adsorption of water molecules and polar ions into their structure, a phenomenon termed the swelling property. Clay's surfaces may be modified with specific materials to enhance their affinity and compatibility with certain pollutants, particularly for adsorption purposes [5].

NCs are categorized into different types based on their structural configuration, primarily focusing on the arrangement of tetrahedral and octahedral sheets. The 1:1 clay, such as kaolinite, consists of one tetrahedral sheet linked to one octahedral sheet, forming a simple layer structure (Fig. S1). These clays are generally non-expansive, with minimal interlayer space, making them relatively stable with low cation exchange capacity (CEC). The 2:1 type, including montmorillonite and illite, features two tetrahedral sheets sandwiching one octahedral sheet (Fig. S1). This configuration creates a substantial structure with a significant interlayer space that can accommodate water and cations, leading to higher CEC and swelling properties, which are advantageous in adsorption applications. However, the 2:1:1 type, such as chlorite, incorporates an additional octahedral sheet between the layers of tetrahedral-octahedral-tetrahedral units (Fig. S1). This extra sheet further stabilizes the structure, reducing the swelling tendency but retaining some level of interlayer space and moderate CEC. In addition to this classification, clay minerals may exist as elongated fibrous structures characterized by ribbon-like layers of two tetrahedral sheets linked by a central octahedral sheet sharing oxygen atoms, yielding a trough and channel structure [7,10]. Each type of clay, with its distinct structure, offers specific advantages for various industrial and environmental applications, particularly in water treatment. Fig. S1 illustrates the types of clays according to their structure.

2.1. Kaolinite

Kaolin, referred to as "Chinese clay," comprises a range of clay minerals, including kaolinite, halloysite, dickite, and nacrite, with kaolinite being the predominant NC. The general formula for members belonging to this group can be represented by $Al_2Si_2O_5(OH)_4{\cdot}nH_2O$ (n = 0–4) [10]. Kaolinite is a 1:1 clay (Fig. 1(a)), lacks swelling behavior, displays a white coloration, and its composition is characterized by a higher proportion of alumina compared to silica. The structure consists of stacked pseudohexagonal platelets, each platelet is an arrangement of two sheets, a tetrahedral sheet of silicon with an octahedral sheet of aluminum (Fig. 1(a)), one above the other [7,12]. Kaolinite NC exhibits a low cation exchange capacity and features highly robust bonds between its layers. These characteristics pose challenges for the intercalation of other molecules or polymer chains, indicating limited suitability for nanocomposite formation.

2.2. Halloysite

Halloysite represents a naturally occurring 1:1 clay (Fig. 1(b)), primarily sourced from New Zealand. The properties of this NC are dictated mainly by its geological origin. Halloysite exhibits inert characteristics, and its biocompatibility renders it intriguing for applications in dye adsorption and the biosorption of heavy metals [5,10,12]. Halloysite ($Al_2Si_2O_5(OH)_4.nH_2O$) has a composition similar to kaolinite, except for the nanotubes hollow-cylindrical structure and the existence of an extra monolayer of water between the layers [13]. Halloysite exhibits a two-layer tubular structure, with nanotubes with an external diameter of 50–100 nm, an internal diameter of 10–30 nm, and a length reaching up to 2000 nm (Fig. 1(b)). Halloysite nanotubes are part of the aluminosilicate group, exhibiting a hollow tubular structure resulting from alternating octahedral and tetrahedral layers within the material [13,14]. The external surface primarily consists of SiO_2 and bears a negative charge attributable to the lower density of hydroxyl groups

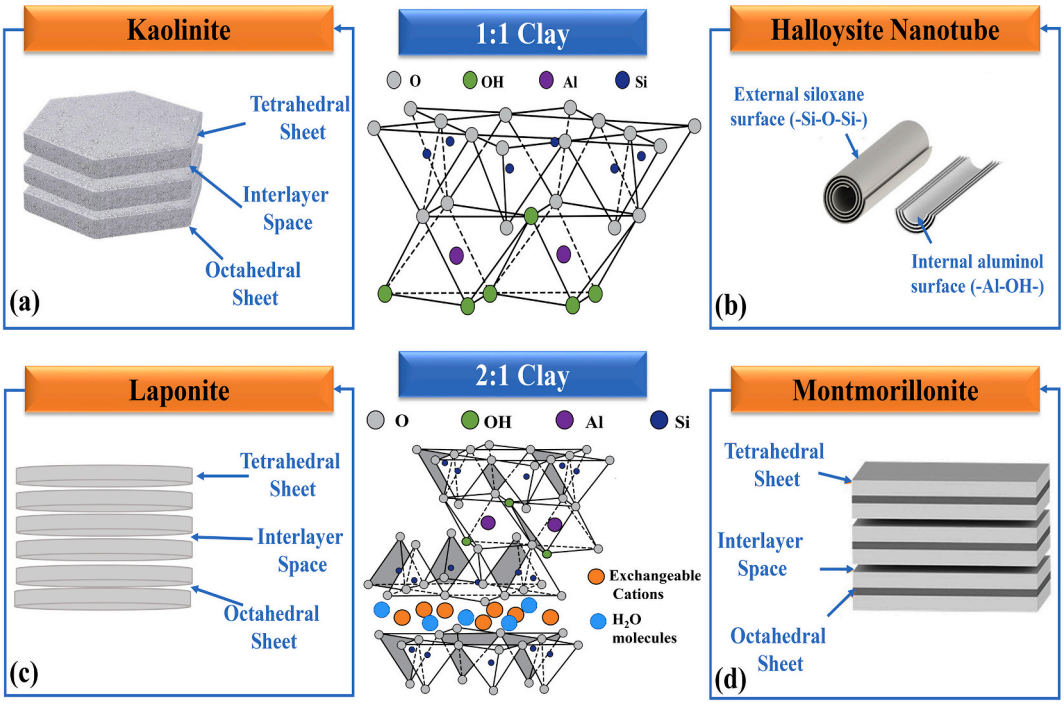

Fig. 1. The structure of 1:1 and 2:1 clay: (a) kaolinite, (b) halloysite clay nanotube, (c) laponite, and (d) montmorillonite.

(SiOH). In contrast, the internal surface carries a positive charge, owing to a higher abundance of hydroxyl groups (Al-OH), and is predominantly composed of Al_2O_3. Halloysite adopts a cylindrical shape, a consequence of the mismatch in layer alignment. Recently, halloysite utilization has surged due to its cylindrical morphology, substantial surface area-to-volume ratio, thermal stability, controlled release capabilities, and cost-effectiveness. Halloysites offer a notable advantage over other layered structures due to the presence of weak secondary interactions between nanotubes. This characteristic enables their dispersion within a polymeric matrix, facilitating interaction with polymeric chains and fostering strong bonding. Also, halloysites exhibit greater hydrophilicity than other clays, allowing for effective dispersion in water. However, a drawback of this natural material is its high concentration of impurities, necessitating their removal to enhance its efficacy as an adsorbent agent [5].

2.3. Laponite

Laponite is a hectorite variant manufactured commercially, having a chemical composition expressed as $Na^{+}_{0,7}[(Si_8Mg_{5,5}Li_{0,3})O_{20}(OH)_4]^{-0,7}$ [15], closely resembles the structure and composition of hectorite, with a chemical formula $Na_{0,3}(Mg, Li)_3Si_4O_{10}(OH)_2$. Laponite comprises basic units composed of layered hydrated magnesium silicate platelets (Fig. 1(c)). It exhibits a relatively small particle size, with a diameter typically ranging around 30 nm and a thickness of approximately 1 nm. Each cell comprises six octahedral sheets coordinated with Mg^{2+} ions. These sheets are between two layers of four tetrahedral sheets coordinated with Si^{4+} ions. The positive charge arises from oxides and hydroxyl groups, while anions result from isomorphic substitution of cations (Fig. 1(c)).

2.4. Montmorillonite

Montmorillonite is classified as a layered silicate, capable of incorporating various minerals such as talc, saponite, and pyrophyllite (Fig. 1 (d)). It represents the most prevalent mineral within the smectite group. Its chemical composition predominantly comprises SiO_2, with minor amounts of Al_2O_3 and Fe_2O_3. This abundant natural clay is economically viable and yields favorable adsorption outcomes, attributed to its notable cation exchange capacity [5,10]. The microstructure of montmorillonite exhibits a platelet morphology and comprises two layers: one layer consists of tetrahedral silicon, while the other consists of octahedral aluminum oxide. This arrangement forms a 2:1 dioctahedral layer with a broad dehydroxylation temperature range of 500–700 °C. The particle size of montmorillonite can range from 2 μm to 0.1 μm and may be smaller when exfoliated, with an average diameter of 1 μm [5,12]. Montmorillonite finds extensive application in fabricating nanocomposites with polymers, owing to its ready availability, established intercalation or exfoliation mechanisms, substantial surface area, and pronounced surface reactivity. It is worth mentioning that water molecules easily penetrate it. Therefore, the network expands significantly, and the distance between the layers tends to increase, which is beneficial for the penetration of polymer chains [10,12].

3. Nanoclay synthesis methods

The physical-chemical properties of clays can be improved through modification methods. Technological advances have allowed the diversification of clay modification methods, which include surface modification methods and methods for preparing clay/polymer nanocomposites. In general, modifications to clays include chemical and physical modifications that involve using and handling the properties of clay minerals to varying degrees, from a simple ion exchange to a drastic change in their structure with the corresponding formation in nanocomposites. These methods can be combined to optimize the preparation of clays to incorporate clay into a host matrix. It is necessary to modify the surface of the clays since many polymers (hydrophobic character) are incompatible with clays (hydrophilic character) [16,17]. This section outlines the synthesis and modification methods of NCs, emphasizing their role in water treatment. It covers common techniques such as acid activation, organo-functionalization, silylation, pillaring, and polymerization, which enhance the adsorption capabilities of NCs by altering their surface chemistry and structural properties.

3.1. Acid activation

The acid activation process employs hydrochloric or sulfuric acid to improve clay's physicochemical characteristics and is considered a well-known modification method. The mechanism is based on ionic exchange between interlayer cations (Na^+ or Ca^{2+}) by H^+. Through this process, the cations within the crystalline lamellae, such as Al^{3+} in the octahedral sheets, are removed from their positions, creating large pores within the structure. Subsequently, this leads to forming amorphous silicon oxide (SiO_4) sheets [18]. Recent studies have shown that acid activation of bentonite using hydrochloric or sulfuric acid yields materials with enhanced surface areas, heightened acidity, increased porosity, and improved thermal stability [11,17,18]. This process can augment the surface area of raw clays by up to fivefold and potentially eliminate various mineral impurities [19]. Fu et al. [20] employed acid leaching on natural halloysite nanotubes (HNTs) to prepare mesoporous silica nanotubes (MNTs). The procedure was performed via clay pretreatment (emulsion dispersion, filtration, washing with distilled water, and drying for 8 h at 80 °C). The dried HNTs (3 g) were treated with 750 mL of hydrochloric acid (HCl) solution at various concentrations (1–6 M) and temperatures (50–100 °C), with constant improvement for different periods (0.5 h–10 days). After that, the suspension was filtered, washed, and dried again. The treatment resulted in modified HNTs with larger diameters, uniform mesopores, and adsorbent species preserved in the outer halloysite layer [20].

3.2. Organo-functionalization

Organo-functionalization relies on the interaction mechanisms occurring between clay minerals and organic compounds. This process involves modifying the surface of clay minerals by incorporating organic functional groups, thereby altering their properties and enhancing their compatibility with organic materials or polymers [21–24]. Organo-functionalization enhances the interfacial interactions between clay minerals and organic matrices, improving performance in various applications such as composite materials, adsorbents, and catalysts [25]. This interaction decreases the energy of the clay mineral, enhancing its compatibility with organic polymers. Consequently, it yields a clay-polymer compound with enhanced mechanical, physical, and chemical properties. Organophilic clays are typically synthesized through cation exchange or solid-state reactions [26].

In the ion exchange method, a precursor solution containing organic cations, mainly quaternary ammonium surfactants, is placed in contact with clay with ion exchange capacity so that an ion exchange reaction occurs, which generally develops in the intermediate layer of the NC. The mechanism of organophilization by ion exchange is based on contact between aqueous clay suspensions and solutions of quaternary ammonium surfactants in the suspension. The outcome is a wet cake that yields organophilic clay when subjected to subsequent processes like filtration and oven drying [19]. Breakwell et al. [27] used 12 g of bentonite (mainly in the form of Na+) dispersed in 350 cm^3 of distilled water. The suspension was decanted, the residue was separated, dried and weighed. Hexadecyltrimethylammonium chloride was added to the remaining clay, which was stirred for one week. The product was filtered, washed, and air-dried. Ion exchange was confirmed in the filtered material (Na^+, by atomic absorption), indicating 100 % ion exchange. However, organic molecules are incorporated into clays without solvents in the solid-state reaction method. Dry organophilization protocols described in the scientific literature involve high-shear mixers [27], mechanochemical processes [28], and ion-dipole interaction [29].

After undergoing organo-functionalization, the clays are designated as organophilized clays. They typically exhibit enhanced attributes, including heightened nonpolar characteristics. This enhancement enables their integration into organic media, facilitating the formation of clay-organic compound complexes. These complexes find applications in cosmetics, paints based on organic solvents, non-polar polymers, and lubricants [22,26]. Baruel et al. [22] observed that substituting sodium cations with organic cations typically increases the basal distance. The authors noted that the extent of this increase correlates with the size of the organic salt chain. This phenomenon can be verified using analytical techniques such as X-ray diffraction (XRD).

3.3. Silylation

Another method investigated for enhancing the surface properties of clays involves silylation. Fig. S2 illustrates the interaction's locations between silane groups and clays. An organosilane compound containing two reactive groups is employed during the silylation process. This compound reacts with the hydroxyl groups on the clay surface, which leads to organic functional groups' attachment [30,31]. This modification alters the surface chemistry of the clay, resulting in improved characteristics such as increased hydrophobicity or compatibility with organic materials [32]. Silanes have the general formula R-(CH_2)n-Si-X_3, where R represents a non-hydrolyzable organic group and X, is a hydrolyzable group. The R group interacts with the polymeric matrix, and X interacts with the organic substrate, producing silanol and forming covalent siloxane bonds (Fig. S2). The functionalization of the clay surface improves the interaction with the medium in which the clay is incorporated as the silane group interacts simultaneously with the clay and the polymeric matrix, promoting their union. Covalent bonds are formed between the clay and silanes, which makes the bond, unlike cation exchange [22,33].

The methodology proposed by Di Gianni et al. [34] uses alkoxysilanes and explores the OH reactive sites in the structure of sodium montmorillonite (Cloisite Na^+) [34]. The procedure was performed by mixing 400 mL of an EtOH/H_2O (75:25) solution, 1.5 g sodium montmorillonite and excess (5 g) of glycidyl-propyltriethoxysilane (GPTS) under stirring for 4 h at 80 °C. Then, the mixture was filtered, washed with ethanol, and dried in an oven at 80 °C overnight. The method proved to be efficient for functionalizing the surface of clay mineral platelets using OH groups as active sites that may be present in a) edges, b) spaces between layers, and c) NC surfaces, as shown in Fig. S2. Modifying the surface of clay particles with silanes gives the materials better mechanical properties and can also increase the distance between layers when silanes are inserted into the interlayer layer [35].

3.4. Pillaring

The pillarization process in clays involves the introduction of pillars or organic molecules into the interlayer spaces of layered clay minerals, such as montmorillonite or kaolinite (Fig. 2). This process aims to enhance the structural stability and expand the interlayer distance of the clay mineral, thereby modifying its properties for various applications (Fig. 2). This method allows the production of a thermally stable micro and/or mesoporous material, without destroying the lamellar structure of the clay during the process. Typically, the pillarization process begins with the intercalation of a swelling agent, which expands the interlayer spaces of the clay. Subsequently, pillars or organic molecules are introduced into these expanded spaces, often through ion exchange or covalent bonding [36]. The incorporation of pillars reinforces the clay structure, preventing collapse and improving its mechanical strength. Moreover, pillarization can impart specific functionalities to the clay, such as increased adsorption capacity, catalytic activity, or selective molecular sieving properties [37,38]. The process unfolds through several sequential steps: initially, the clay undergoes swelling with water, enabling the expansion of its interlayer spaces (Fig. 2). Following this, there is an exchange of interlayer cations with partially hydrated oligomeric or polymeric metal complexes, thereby enhancing the separation between the clay layers. Subsequently, drying and calcination transform the polyoxocation precursors into metallic oxide pillars. These metallic oxide pillars then undergo covalent bonding to the clay's

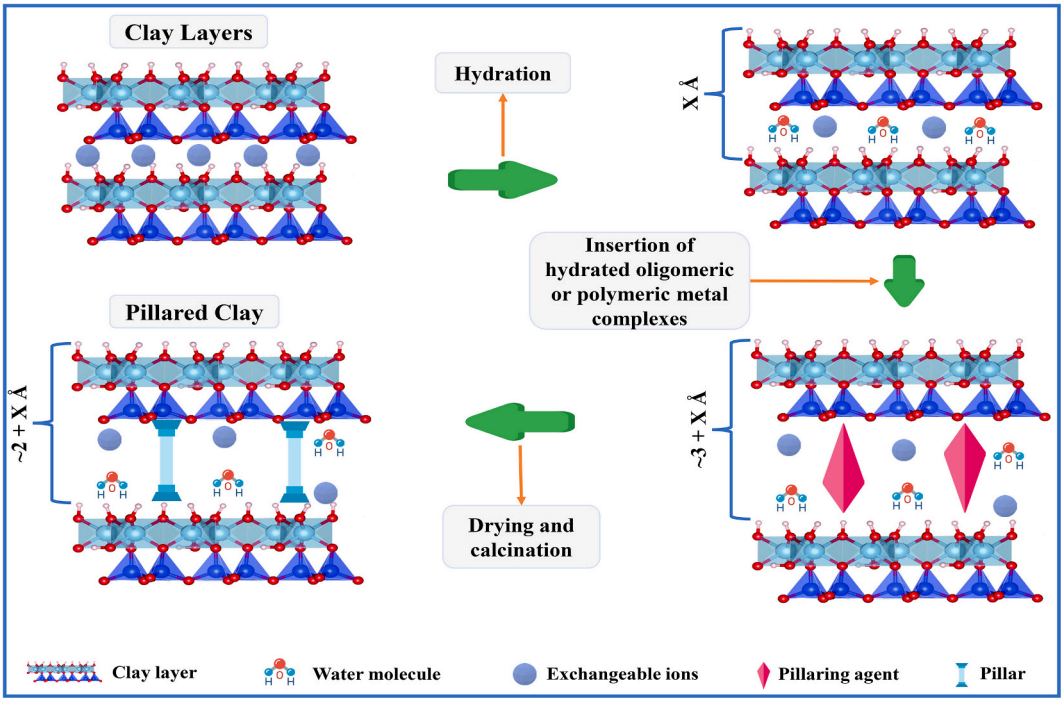

Fig. 2. The pillarization process clay during different stages of pillaring.

tetrahedral sheets, ensuring the permanent separation of the layers [19].

Pillarized clays generally have high surface areas (50 to 200 m^2/g), pore volumes, and adjustable pore sizes resulting from the intercalation of bulky species in the interlayer spaces. Due to their improved characteristics, they are widely used in heterogeneous catalysis, as in addition to these structural characteristics, they provide strong surface acidity and pillars of catalytically active metal oxides. However, one of the prerequisites for pyramidization is that the starting material has expansion and ion exchange properties, such as smectites and vermiculites [19]. Desai et al. [39] schematized the clay pillarization process using chromium (Cr) as a pillaring agent [39]. The process involves two main steps: intercalation of pillaring agents followed by calcination. In the intercalation step, the raw clay was mixed with Cr polycation solution at room temperature for 2 h and allowed to age for another 22 h. In the ultrasound-assisted method, the raw clay was added to the Cr polycation solution and sonicated at a frequency of 35 kHz for 30 min. In this calcination step, the naturally occurring cations in the clay are replaced by Cr cations. For the procedure, previously oven-dried polycations were converted into metal oxide pillars by heat treatment (calcination at 500 °C for 2 h). The results demonstrated that the Cr incorporated into the pillared clay matrix remained stable after the adsorption processes of the Acid Blue 74 and Basic Orange 2 dyes. Moreover, the ultrasound accelerated the desorption time of the Basic Orange 2 dye from the clay by 48 times and allowed its reuse in four more cycles without an appreciable drop in capacity [39].

3.5. Polymerization

The polymerization process in clays involves the incorporation of polymer chains into the interlayer spaces or onto the surface of clay minerals (Fig. S3). This process aims to enhance the mechanical, thermal, and chemical properties of clay-based composites for various applications. Typically, polymerization begins with the dispersion of clay minerals in a monomer solution or melt, followed by the initiation of polymerization reactions. Polymer chains then insert within the clay's interlayer spaces or on its surface through grafting or copolymerization reactions [40,41]. The polymer chains can effectively intercalate between the clay layers (Fig. S3), leading to the formation of polymer-clay nanocomposites. This intercalation imparts unique properties to the resulting materials, including improved mechanical strength, thermal stability, flame retardancy, and barrier properties. Moreover, the presence of clay nanoparticles can influence the polymerization kinetics and morphology of the resulting composite materials. Generally, NC particles are usually incorporated into polymer matrices using different processing techniques, such as solution-induced intercalation, in situ polymerization, Sol-Gel templating, or melt processing [16,17].

The solution-induced intercalation method is an indirect way of preparing NC/polymer nanocomposites. In this method, a solvent is used to make the polymer soluble. The clay is dispersed in the polymeric solution, and its lamellae swell, enabling the incorporation of the polymer and solvent mixture (intercalation) (Fig. S3). In the final stage, the solvent used is evaporated, after which the interspersed sheets come together to produce nanocomposites. Thus, the three stages of nanocomposites preparation using the solution-induced intercalation method are: 1) dispersion of the clay in a polymeric solution, which can be used through stirring, reflux, shear mixing, and ultrasonication, 2) controlled removal of the solvent, and 3) actual formation of the nanocomposite [16,42]. Buruga et al. [43] synthesized two composites of polymethyl methacrylate (PMMA) and polystyrene (PS) based on halloysite nanotubes (HNTs). To synthesize HNT-polymer nanocomposites, 30 mL of toluene was added to 0.15 g of HNTs (5 wt%). The mixture was stirred for 60 min, followed by sonication for 30 min. Then, 3 g of polystyrene or PMMA was added to the toluene containing HNTs, subjected to stirring and sonication again, forming HNT-PS or HNT-PMMA nanocomposites.

In melt mixing, nanocomposites are prepared by directly mixing between clay and polymer and heated to a temperature above its softening point without solvents. If there is compatibility between the polymer and the clay surface, the polymer will penetrate between the clay layers, forming the corresponding nanocomposites. The fusion mixing method can basically follow two routes: a) static fusion method, carried out in the presence of vacuum and with a transition temperature of 50 °C (without mixing), and b) dynamic fusion method, carried out in the presence of inert gas [16,17,44,45]. Narro-Céspedes et al. [46] used sodium montmorillonite NCs modified with methyl methacrylate (Na^+-MMT/MMA) and styrene (Na^+-MMT/St) by plasma polymerization.

These modified NCs were used as reinforcement for polystyrene (PS) nanocomposites that were prepared by melt mixing. First, the PS was introduced into the Brabender chamber, after its melting, 1.5 g of pure Na^+-MMT and 1.5 g modified Na^+-MMT (Na^+-MMT/MMA and Na^+-MMT/St) were introduced and mixed for 10 min. Then, the nanocomposites were extracted, ground, and molded. The PS/Na^+-MMT nanocomposites were prepared with a concentration of 3 wt% Na^+-MMT and 97 % PS.

In the in-situ polymerization method, a polymer precursor or a monomer is inserted between the clay layers. For the preparation of clays/polymers, three processing steps are required: 1) modification of the clay surface through the use of surfactants to make it compatible with the polymer, 2) intercalation of the monomer in the presence of surfactants, and 3) polymerization, with the formation of a long nanocomposite chain [16]. Briefly, the dispersion of clays in polymeric matrices can result in three different morphological configurations: immiscible, intercalated, and exfoliated, as shown in Fig. S3 [16,47]. In the immiscible state, the clay particles maintain their original stack (Fig. S3), without the presence of polymers between their layers. Many authors do not consider this as a nanocomposite and argued that the improvement in the material's properties is limited. On the other hand, in the intercalated state, the polymer matrix is inserted between the clay layers, causing a space of 2 to 3 nm between the layers (Fig. S3). However, in the exfoliated state, the clay layers separate, generally 20 nm or more apart (Fig. S3). However, this classification is not rigid, since it is possible to find partially intercalated and exfoliated nanocomposites [16,17,48]. These three morphologies are the result of the dispersion state of the NC, the degree of separation of the silicate layers, and the penetration of the polymer between them, which may vary depending on the type of clay, method of modifying the clay surface, method of processing the clay/polymer composite, type of polymer matrix, fraction of clay incorporated in the polymer and clay/polymer interaction. These different parameters influence and define the properties of the nanocomposite materials formed [16,17].

The main way of differentiating between the immiscible, intercalated, and exfoliated states is to verify the variation in the distance between the clay lamellae (Fig. S3). To obtain this information on the morphological classification of NCs and verify the occurrence of intercalation, different techniques can be used, such as scanning electron microscopy (SEM), X-ray diffraction (XRD), and transmission electron microscopy (TEM) [16]. Baniasadi et al. [49] studied the morphological properties of polypropylene/clay nanocomposites (PPCNs) prepared by in situ polymerization. The procedure used performed the polymerization of propylene in hexane with the Buchi type reactor (1 L) at a pressure of 4 bar and a temperature not exceeding 60 °C, using the reagents triisobutylaluminum and dimethoxymethylcyclohexyl silane as co-catalyst and external donor, respectively. At the end of the polymerization period, the polymer was washed several times with ethanol, then filtered and dried in a vacuum oven at 70 °C for 24 h. The authors identified through XRD analysis that the basal spacing of the clay has a layered structure with a d-spacing of 1.15 nm, while XRD analysis of the PPCNs composite did not show any peak, which was attributed to polymerization generating exfoliated composites. From these spacings, the success of the modification in the clay structure can be observed. The exfoliation of the clay lamellae was confirmed by TEM micrographs, which indicated that the material presented a uniform distribution and exfoliated structure [49]. Furthermore, a prospective survey of the technologies involved in clay and NC modification methods was carried out. Fig. S4(a) prospective mapping of modification methods applied to NCs.

4. Characterization of nanoclays

The advancements in characterization techniques hold paramount importance in comprehending the nanoscale structure and interfacial interactions among nanostructured constituents. The insights gleaned from such characterizations facilitate the exploration of novel applications for synthetic NCs, pillarized clay minerals, porous clay heterostructures, and nanocomposites. Consequently, the modification of NCs can be tailored to enhance their affinity for specific contaminants, thereby facilitating the adsorption performance for various pollutants. This section discusses the importance of characterization techniques in synthesizing and applying NCs for water treatment. It covers key methods such as surface area analysis, zeta potential measurement, infrared spectroscopy, and X-ray and electron diffraction, which are essential for understanding the structural and chemical properties of NCs. Table S2 summarizes the general characteristics of NCs according to their classifications. Surface area, porosity, and pore size distribution are among the most essential configurations of porous materials and NCs, as they control surface phenomena and directly affect elastic and mechanical behavior, fluid movement and flow, etc. [50]. The specific surface area is generally evaluated through nitrogen (N_2) adsorption isotherms at 77 K.

In a clay-water suspension, solid particles develop charges at the solid-liquid interface due to the dissociation or adsorption of ions from the solution, forming an electrical potential on the surface of the particles and attracting a portion of oppositely charged ions present in the medium [51,52]. The potential difference between these two layers is called "zeta potential". While, the *zero-charge potential* (ZCP) is the pH value at which the surface charges of a clay or solid are in equilibrium, making it possible to predict the effect of pH on the phenomena and processes involving adsorption [53,54]. Kryuchkova et al. [55] studied the removal of carbamazepine, ibuprofen, and paracetamol through an adsorptive process with Montmorillonite NC. According to the zeta potential results, the two NCs presented opposite charges, with commercial montmorillonite (MMT) showing a negative charge and tertiary ammonium salts (MMT-STA) presenting a positive charge. As the drugs studied have a negative charge, the comparative analysis between natural montmorillonite and modified montmorillonite resulted in MMT-STA having better adsorption properties [55]. Zhang et al. [56] observed that the controlled release of a drug could influence the type of bonding, charge, and pH_{ZCP} of NC. An increase in the release rate was observed due to the decrease in electrostatic interactions with the carrier surface [56]. Ribeiro et al. [57] observed that clay's surface load and pH_{ZCP} are influenced by the soil's balance of mineral and organic components. Iron and aluminum oxides elevate positive charges and pH_{ZCP}, while organic matter and silicate clay minerals like kaolinite augment negative charges and lower pH_{ZCP} [57].

Infrared spectroscopy (IR) is used to identify the chemical bonds and functional groups present in NCs. This method analyzes the vibrations of tetrahedral and octahedral units in the lamellar layer, hydroxyls, and other possible organomaterials. Like the thermal stability of NC, an IR spectrum is a fingerprint for its identification. On the other hand, X-ray and electron diffraction techniques are pivotal in discerning the crystalline and atomic structures of clay minerals [10]. These techniques are instrumental in determining the primary structural and crystalline features of NCs and nanocomposites, thereby enabling the assessment of the extent of intercalation and exfoliation of clay nanoparticles. Zhang and Wang [58] studied the adsorption and desorption of Nickel (II) ions from an aqueous solution through the Lignocellulose/Montmorillonite composite. The authors confirmed the formation of the flocculated-intercalated nanostructure through the XRD technique. Pure Montmorillonite presents a typical diffraction peak at $2\theta = 5.83^\circ$ and, with the intercalation of Lignocellulose, the intensity of this characteristic peak decreased, even disappearing, indicating intercalation and resulting in the destruction of the Montmorillonite structure [58]. Ramanayaka et al. [59] evaluated the affinity of the natural halloysite NC in the drug adsorption from an aqueous solution, and confirmation of the interaction between the oxytetracycline and NC was carried out using FTIR and XRD techniques [59].

Different microscopy techniques are used to characterize NCs and nanostructured materials. Other electron microscopy techniques, such

as scanning electron microscope (SEM) and transmission electron microscope (TEM), are used to verify the topology of these materials. Transmission electron microscopy (TEM) enables the observation of crystalline defects, including stacking faults, which are not discernible through optical microscopy or scanning electron microscopy (SEM). Moreover, TEM allows for the analysis of nanometer-scale precipitates, offering precise insight into the dispersion of NCs within the polymer matrix. This capability underscores the utility of TEM in investigating how different types of polymers influence the dispersibility of clays. Beyond elucidating nanomaterials' shape, size, and distribution, TEM results furnish valuable information regarding uniformity, internal and external diameters, and other pertinent parameters [60,61]. Table S3 summarizes some characterization results of NCs.

5. Adsorption performance of nanoclays

The adsorption process is widely employed for pollutant removal from water owing to its numerous benefits, including high efficiency, cost-effectiveness, ease of operation, and the availability of diverse precursors [62,63]. The adsorption of pollutants by NCs represents a promising and environmentally friendly approach to water remediation. NCs possess a high surface area, which is often characterized by its layered structure, providing numerous active sites for pollutant adsorption. The adsorption process involves the interaction between the surface functionalities of the adsorbent and the target pollutants, including heavy metals, dyes, nutrients, pesticides, and emerging contaminants [64]. The adsorption capacity and efficiency of NC are influenced by several factors, such as the type of NC, particle size, surface modification, and the physicochemical properties of the pollutants and the surrounding aqueous environment (Fig. 3). The adsorption of pollutants onto NCs occurs at various surface locations dictated by the diverse characteristics of the NC structure. The layered and porous nature of NCs presents an array of active sites for adsorption on both the external surfaces and within interlayer spaces (Fig. 3). Pollutants can interact with the edges and external surfaces of NC, facilitated by electrostatic interaction and chemical bonding, allowing for swift access to these binding sites [65]. Additionally, the interlayer spaces, possessing a high surface area, present binding sites for pollutants, leading to their inclusion within the NC structure (Fig. 3). Additionally, the versatility of NC opens up opportunities for developing novel adsorption materials and technologies in the quest for sustainable water quality management. Traditionally, batch-mode experiments are first employed to evaluate the efficacy of NC-based adsorbents in removing contaminants from their matrices. The majority of significant advancement and research in the adsorption process may be accomplished on a lab-scale using batch or fixed-bed (continuous flow) mode. Investigating adsorption data characterized by fixed bed importantly highlights more helpful insights about adsorption dynamics, which is required for scaling up the adsorption process.

5.1. Heavy metals

The deleterious influence of heavy metals on water quality is evident through their contamination of aquatic ecosystems, posing risks to aquatic life and human consumers of affected water sources [66]. Heavy metals, including lead (Pb), chromium (Cr), cadmium (Cd), mercury (Hg), and arsenic (As), are highly toxic and pose a severe threat to the environment and human health. Adsorption of heavy metals by NC and NC composites is a topic of significant interest in water pollution remediation. Due to its high surface area and layered structure, NC exhibits a remarkable capacity to adsorb heavy metal ions from aqueous solutions. The adsorption process involves binding heavy metal cations to the negatively charged surfaces of NC through electrostatic interactions and ion exchange, resulting in the formation of stable surface complexes.

The selection of NC type, particle size, and surface modification is

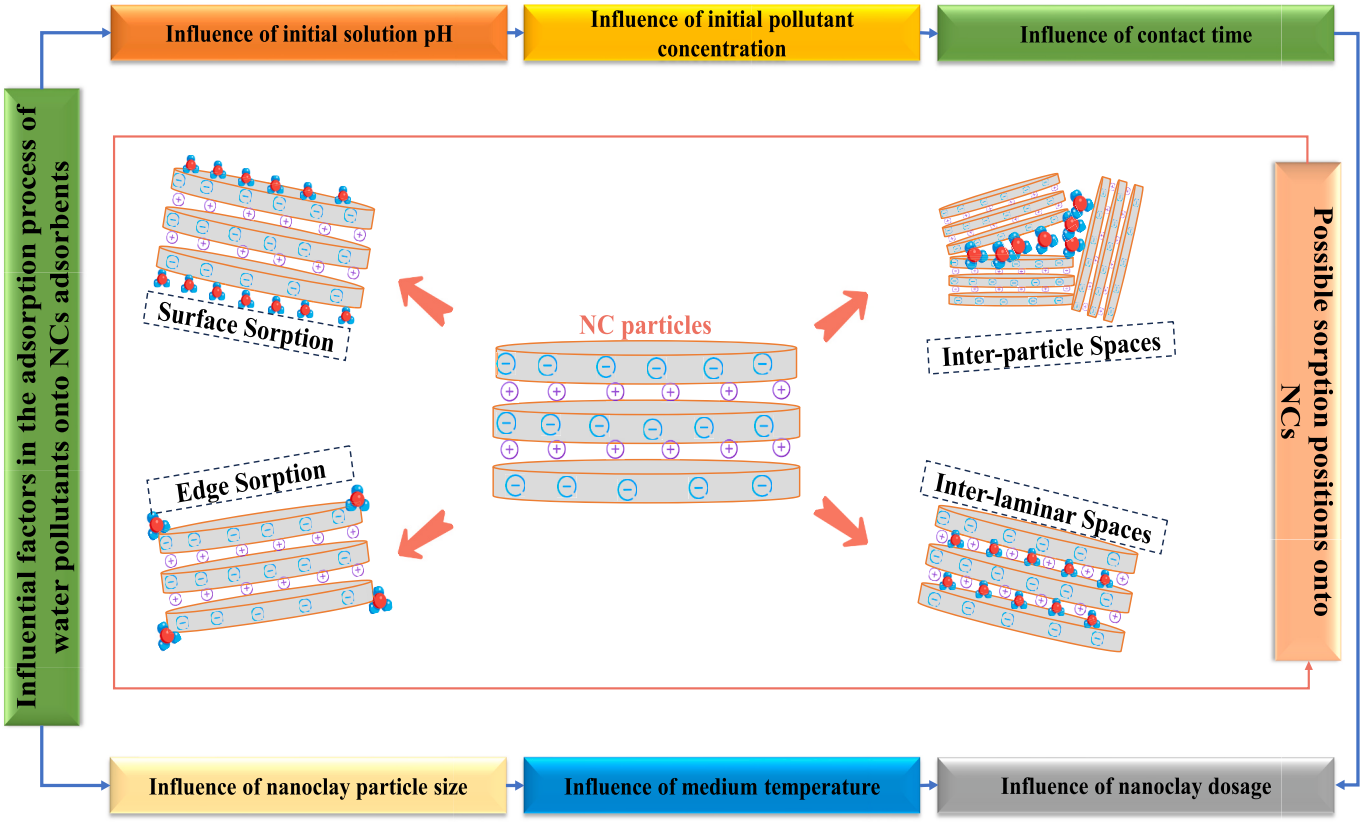

Fig. 3. The operational parameters affecting the adsorption process and the possible sorption positions onto NCs.

critical in determining the efficiency and selectivity of heavy metal adsorption by NCs. Several research studies used NCs and NC composites to eliminate heavy metals (such as Pb, Cd, Hg, As, etc.) from aqueous solutions. Modified Halloysite NC was utilized to remove As(III) ions from water [67]. This modified NC demonstrated a maximum adsorption capacity of 8.67 mg/g, under optimized conditions (1 g/L; 90 min; pH 8) in distilled water. Furthermore, the montmorillonite-k_{10} (MMT-K_{10}) NC was assessed using the Response Surface Methodology (RSM) method towards the removal of Pb(II) ions [68]. The outcomes from RSM indicated a conformity of the experimental data to the quadratic model, as evidenced by the notably high regression coefficient value (R^2 = 0.9903) and the statistically insignificant lack of fit (0.2426), affirming the adequacy and validity of the Quadratic model. The Langmuir mono-layer maximum sorption capacity of MMT-K_{10} was found to be 40.86 mg/g, and pseudo-2nd order kinetic model exhibited the best fitting of the data. Furthermore, hydrogel composites consisting of chitosan crosslinked with NC particles were synthesized using gamma irradiation at a dose of 25 kGy to remove Cr(VI) and Pb(II) from water [69]. The sorption data of the synthesized composite revealed sorption capacities of 125 mg/g and 205 mg/g for Pb(II) and Cr(VI), respectively (Table 1), at an alkaline medium within 90 min. Moreover, the kinetic modeling data indicated that the Pb(II) and Cr(VI) sorption followed pseudo-1st order kinetic model with acceptable regeneration ability for three successive cycles [69]. Wang et al. fabricated two-dimensional (2D) NC (ultrathin Janus serpentine) nanosheets to get insight into the facet-dependent adsorption mechanism of Cd(II) and Pb(II) [70]. The fabricated 2D NC nanosheets demonstrated four folds higher sorption performance for Cd(II) (579.20 μmol/g) and Pb(II) (556.50 μmol/g) compared to raw serpentine powders (145.9 μmol/g) for Cd(II) and (146.2 μmol/g) for Pb(II). The authors reported that the Cd(II) and Pb (II) sorption onto the fabricated nanosheets exhibited a facet-dependent feature. Moreover, the mechanistic studies revealed that the adsorbed amount on the Si—O plane was substantially less than the Mg–OH plane. Table 1 summarizes various types of NC and NC composites used to remove heavy metals from water.

A comparison was conducted between the adsorption capacities of NCs and other adsorbents for Pb(II) removal to evaluate the performance of NCs [71–80]. This analysis highlights the relative efficiency of NCs in heavy metal adsorption compared to alternative materials. Fig. 4 (a) illustrates that the adsorption performance of Pb(II) ions varies significantly across different treatment materials and adsorbents when addressing Pb(II) contamination in water. Metal-Organic Framework (MOF-DFSA) exhibits an exceptional adsorption capacity of 349.09 mg/g [72], highlighting its superior efficiency in capturing Pb(II) ions, which positions it as one of the most effective materials for heavy metal removal. However, NCs, particularly functionalized bentonite [75] and nano kaolinite [76], also show competitive performance, with adsorption capacities of 147.05 mg/g and 125.00 mg/g, respectively (Fig. 4 (a)). These values indicate that NCs can effectively adsorb Pb(II) ions, outperforming other common materials like graphene nanosheets (35.70 mg/g) [74] and magnetic magnetite nanoparticles (53.11 mg/g) [80]. Notably, activated nanoclay/hydrocolloid composites achieve an adsorption capacity of 108.14 mg/g [73], further demonstrating the potential of modified NCs in water treatment applications. On the other hand, adsorbents derived from natural waste materials, such as Rosa damascena waste, exhibit a much lower adsorption capacity of 24.90 mg/g [77], underscoring the need for more advanced or modified materials for effective Pb(II) removal. Mesoporous silicas and wood ash/graphene oxide (GO) composites show moderate adsorption capacities of 113.52 [78] mg/g and 47.20 mg/g [79], respectively (Fig. 4(a)), indicating that while they are effective, they may not be as efficient as certain NC-based materials or other advanced adsorbents like MOFs. Furthermore, while MOF-DFSA represents the pinnacle of adsorption capacity for Pb(II) ions, NCs, and their composites offer a promising balance of performance and potential economic feasibility, making them strong candidates for practical applications in water treatment.

5.2. Radionuclides

The proliferation of nuclear technology, as a solution to global energy challenges, has unintentionally led to the release of radioactive contaminants, known as radionuclides, into the environment. These contaminants, originating from sources like nuclear power plants and industrial activities, pose significant ecological hazards. Radionuclides, such as Uranium (U(VI)), Strontium (Sr(II)), and Thorium (Th(IV)), find their way into natural water bodies via industrial wastewater discharge, threatening organisms and ecosystems due to their carcinogenic, radiotoxic, and mutagenic properties [81,82]. NCs are believed to exert a significant influence in mitigating the adverse impacts of released radioactive nuclides (RNs) on the environment. Their properties and compositions suggest potential mechanisms for the containment or sequestration of RNs, contributing to environmental protection efforts [82].

The presence of strontium in wastewater is a significant concern due to its potential environmental and health impacts. Both stable and radioactive forms of strontium can dissolve in water, with stable strontium frequently infiltrating rivers or groundwater as a result of the weathering of limestone or rocks containing high concentrations of celestite [83]. Various studies reported the adsorption of Sr(II) using varied types of clays and NC minerals [84–87]. Most recent research indicates that Sr(II) adsorption is significantly influenced by various factors, including clay composition, type of clay mineral, pH, ionic strength, competitive ions in the medium, and other radionuclides [84–87].

Abdel-Karim et al. [85] reported that the adsorption of Sr(II) on clay sampled at the Inshas burial ground (Egypt), comprising kaolinite, vermiculite, illite, calcite, and plagioclase feldspar, exhibited a notable increase within 20–30 min and attained equilibrium rapidly within 90 min. However, the selectivity of the clay for Sr(II) was found to be lower than Cs(I). The authors reported that with pH increasing within the range of 2–12, there was a corresponding increase in adsorption capacity, mirroring a similar trend observed for Cs(I). The maximum adsorption capacity was found to be 39.683 and 46.296 mg/g for Sr(II) and Cs(I), respectively [85]. Additionally, the decline in adsorption capacity with rising temperature (25–60 °C) suggested an endothermic adsorption process. Further indications pointed out ion exchange as the primary mechanism for Sr(II) adsorption on this clay. Desorption of Sr (II) in 0.5 M HCl was found to be 1.4 times lower compared to Cs(I), indicating Sr(II) had higher retention due to the latter's greater solubility. Moreover, the adsorption of these radionuclides on clay was observed to be partially reversible [85]. However, Wu et al. [88] observed that in micaceous clays like muscovite, biotite, and phlogopite from Hebei province, China, Sr(II) adsorption was influenced differently by pH levels. Muscovite and biotite clays exhibited enhanced Sr(II) adsorption under alkaline conditions (pH > 7), whereas the adsorption capacity of phlogopite increased with rising pH within the range of 2–11 [88].

Uranium (VI) ions can be present in aqueous solutions due to natural and anthropogenic sources, posing potential environmental and human health risks [89]. The speciation of uranium ions in aqueous environments is notably influenced by the solution pH, leading to the formation of diverse complexes with varying compositions [82]. At nearly neutral pH levels, akin to those found in natural water bodies, hydroxo complexes such as UO_2OH^+, $(UO_2)_2(OH)_2^{2+}$, $(UO_2)_3(OH)_4^{2+}$, $(UO_2)_3(OH)_5^+$, and $(UO_2)_4(OH)_7^+$ are prevalent. Conversely, under conditions resembling groundwater, characterized by elevated pH and CO_2 content, neutral or negatively charged hydrolysis byproducts (e.g., $UO_2(OH)_2$, UO_2CO_3, and $(UO_2)_2CO_3(OH)_3^-$) are formed, exhibiting poor adsorption onto negatively charged surfaces [82,90]. Li et al. [91] reported that the adsorption of U(VI) on illite and illite-coated *Paecilomyces catenlannulatus* increased with increasing pH from 1.0 to 7.0, but decreased at pH > 7.5. The adsorption behavior of U(VI) on both illite and illite-coated *P. catenlannulatus* was described using the double diffuse model

Table 1
Nanoclay and nanoclay composites for the removal of heavy metals and radionuclides from aqueous solution.

Adsorbents	Targeted pollutants	Sorption capacity (mg/g)	Optimum conditions				Followed theoretical models
			Concentration (mg/L)	pH	Contact time (min)	Dosage (g/L)	
Nano kaolinite [76]	Zn(II)	100	10.0–120.0	5.5–6.0	60	0.40	Pseudo-second-order, Langmuir
Thiol-lignocellulose sodium bentonite [191]	Zn(II)	357.29	200.0–1710.0	4.84	20	0.34	Pseudo-second-order, Langmuir
Nanoclay/hydrocolloid [73]	Zn(II)	6.47	10.0–250.0	4.50	90	0.10	Pseudo-second-order, Langmuir
Natural clay/Fe–Mn composite [192]	As(V)	120.70	10.0–400.0	3.0–4.0	30	2.00	Pseudo-second-order, Langmuir
Montmorillonite magnetic nanoparticles [193]	As(V)	9.00	0.1–25.0	4.0	360	0.50	Freundlich
Nanoclay/hydrocolloid [73]	As(V)	18.87	10.0–250.0	4.50	90	0.10	Pseudo-second-order, Langmuir
Nanoclay-activated carbon composite beads [194]	As(V)	5.00	5.0–75.0	4.50	720	2.00	Pseudo-second-order, Langmuir
Hydroxyapatite-bentonite clay-cellulose [195]	As(III)	51.00	0.25–180.0	4.0–7.0	5	0.60	Pseudo-first-order, Langmuir
Kaolin/ZnO nano adsorbents [196]	Cr(VI)	117.00	25.0–300.0	5.84	15	0.20	Intra-particle diffusion, Boyd, Jovanovic
Chitosan-NC Hydrogel [69]	Cr(VI)	205.00	25.0–100.0	9.00	90	1.00	Pseudo-first-order, Langmuir
Polyacrylamide/Na- montmorillonite nanocomposites [197]	Ni(II)	322.58	20.0–180.0	6.00	1440	2.00	Langmuir
Nano kaolinite [76]	Ni(II)	111.00	10.0–120.0	5.5–6.0	60	0.40	Pseudo-second-order, Langmuir
Chitosan/NC composites [198]	Ni (II)	144.00	1.0–10.0[a]	–	180	0.30	–
Nanoclay-activated carbon composite beads [194]	Cd(II)	41.30	10.0–300.0	4.50	720	2.00	Pseudo-second-order, Langmuir
Activated NC/hydrocolloid [73]	Cd(II)	7.03	10.0–250.0	4.50	90	0.10	Pseudo-second-order, Langmuir
Chitin-halloysite NC [199]	Cu(II)	4.20	10.0–100.0	6.00	1440	5.00	Langmuir
Dithizone-montmorillonite composite [200]	Hg(II)	100.00	10.0–50.0	4.00	90	0.50	–
Activated NC/hydrocolloid [73]	Pb(II)	108.14	10.0–250.0	4.50	90	0.10	Pseudo-second-order, Langmuir
Chitosan-NC Hydrogel [69]	Pb(II)	125.00	25.0–100.0	8.00	90	1.00	Pseudo-first-order, Langmuir
Alginate/nanoclay ink [164]	Pb(II)	116.00	100.0–600.0	6.00	60	0.25	Pseudo-second-order, Freundlich
Nanoclay-activated carbon composite beads [194]	Pb(II)	74.20	12.0–350.0	4.50	720	2.00	Intra-particle diffusion, Langmuir
Nano kaolinite [76]	Cu(II)	125.00	10.0–120.0	5.5–6.0	60	0.40	Pseudo-second-order, Langmuir
Chitosan/Ag-hydroxyapatite nanocomposite [201]	Cu(II)	40.11	0.50–80.0	7.0	120	0.5	Pseudo-second-order, Langmuir
Fe_3O_4/montmorillonite [202]	Cu(II)	70.92	97.73–602.27	7.0	2	3.20	Pseudo-second-order, Langmuir
Soil Nanoclays [203]	Cu(II)	31.70	10.0–250.0	6.0–8.0	360	2.00	Pseudo-second-order, Langmuir
Chitosan/NC composites [198]	Cu(II)	176.00	1.0–10.0[a]	–	180	0.30	–
Chitosan-minerals-based composites [95]	Cs(I)	1400	50.0–5000.0	7.00	1440	1.00	Pseudo-second-order, Langmuir
Jordanian Bentonite [99]	Th(IV)	108.69	10.0–100.0	3.00	1080	1.00	Pseudo-second-order, Langmuir
Polyacrylamide/Na- montmorillonite [197]	Co(II)	114.94	20.0–180.0	6.00	1440	2.00	Langmuir
Chitosan-minerals-based composites [95]	Co(II)	900.00	50.0–3000.0	5.00	1440	1.00	Pseudo-second-order, Langmuir
Bentonite [204]	Eu(III)	61.0	0.01–190.00	7.00	1440	0.50	Sips and Tóth
Chitosan-minerals-based composites [95]	Eu(III)	18.0	0.01–30.0	5.00	1440	1.00	Pseudo-second-order, Langmuir
Phyllites [204]	Eu(III)	19.50	0.01–190.00	4.50	1440	0.50	Sips and Tóth
ZK06 [205]	Sr(II)	1.90[a]	0.00–3.50[a]	5.00	120	1.00	Pseudo-second-order, Langmuir
ZK09 [205]	Sr(II)	2.42[a]	0.00–3.50[a]	5.00	120	1.00	Pseudo-second-order, Langmuir
Illite [91]	U(VI)	46.73	1.0–20.0	5.00	1440	1.20	Pseudo-second-order, Langmuir
Coated illite [91]	U(VI)	54.35	1.0–20.0	5.00	1440	1.20	Pseudo-second-order, Langmuir
Jordanian Bentonite [99]	U(VI)	62.12	10.0–100.0	3.00	1080	1.00	Pseudo-second-order, Langmuir

[a] mmol/L.

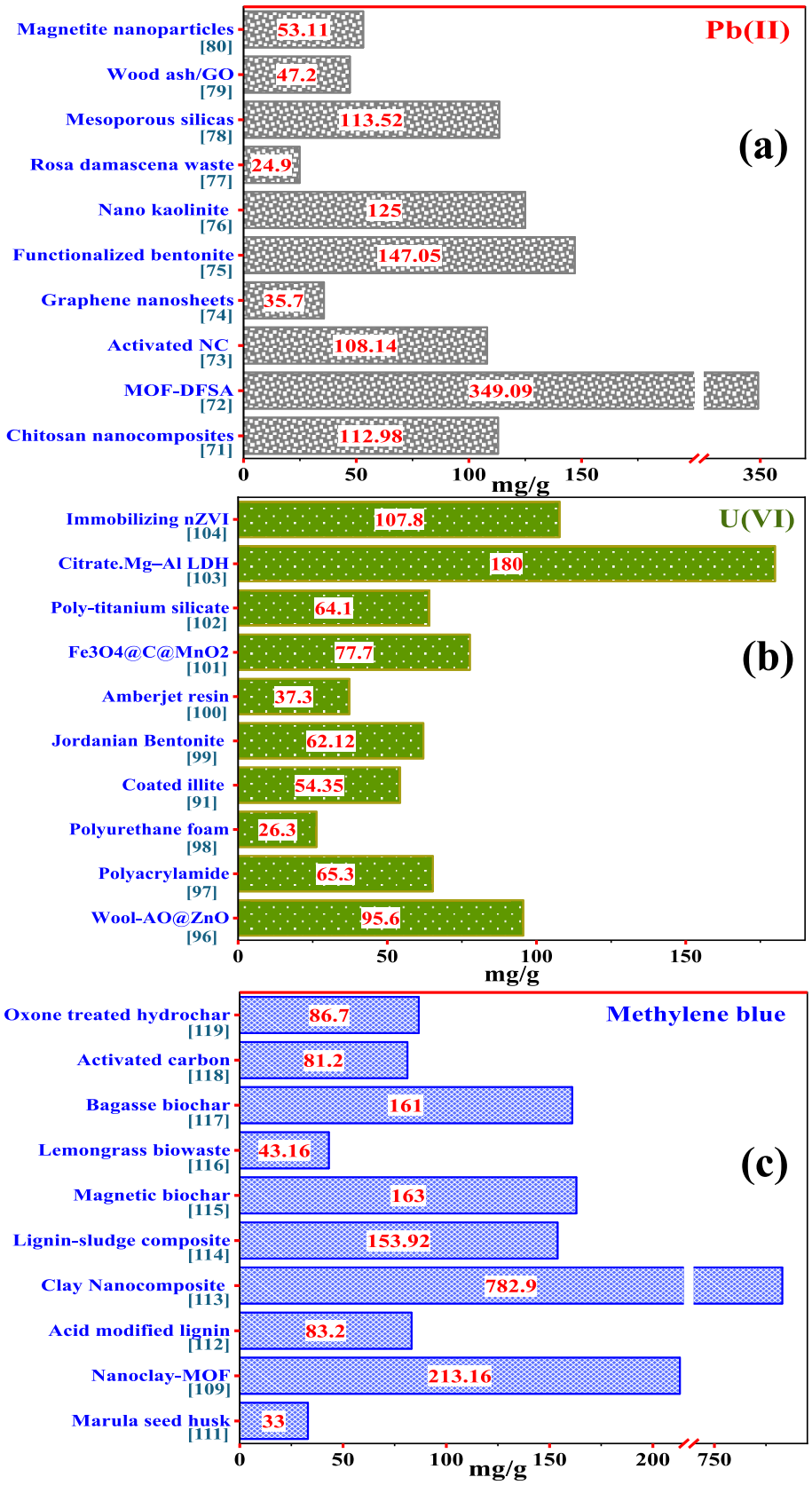

Fig. 4. Comparison of NC and other adsorbents for selective pollutant removal (a) Pb(II) (*Heavy metal*), (b) U(VI) (*Radionuclides*), and (c) Methylene blue (*Dye*). (For interpretation of the references to color in this figure legend, the reader is referred to the web version of this article.)

across varying pH conditions. Experiments dependent on ionic strength indicated outer-sphere surface complexation for U(VI) removal on illite, while inner-sphere surface complexation predominated for U(VI) adsorption onto illite coated *P. catenlannulatus* at pH 5.0–7.0. The maximum adsorption capacity of U(VI) on illite and illite coated *P. catenlannulatus* calculated from the Langmuir model at pH 5.0 and T = 298 K was 46.729 and 54.347 mg/g, respectively (Table 1), demonstrating enhanced adsorption of U(VI) on illite coated *P. catenlannulatus* [91]. Another study reported the effective removal of U(VI) using poly (itaconicacid)-poly(methacrylicacid)-grafted-nanocellulose/ nanobentonite composite [92]. This composite was synthesized by graft copolymerization reaction of methacrylic acid and itaconic acid on nanocellulose/nanobentonite composite using ethyleneglycol dimethacrylate as cross-linker and potassium peroxydisulfate as initiator [92]. The presence of carboxylic groups derived from two monomers enhances the effective adsorptive removal of U(VI), with an optimum pH of 5.5 observed, reaching equilibrium at 120 min. The adsorption process followed the Sips isotherm model with a maximum Langmuir monolayer capacity of 146.55 mg/g at 50 °C, and desorption of adsorbed U(VI) is achieved using 0.1 N HCl [92].

Like U(VI), Europium (Eu(III)) undergoes various chemical transformations depending on the pH of the solution. At low pH levels, it typically exists as $Eu(OH)_2^+$ and $Eu(OH)_3^{2+}$ ions. Conversely, under high pH conditions, such as in the presence of elevated levels of CO_2, europium forms complexes like $Eu(CO_3)^+$ and $Eu(CO_3)^{2-}$ [93]. Furthermore, in acidic environments, H_3O^+ ions compete with Eu^{3+} ions for available binding sites [82]. Another study investigated the Eu(III) adsorption onto smectite and illite mixtures, common clay barriers in waste repositories [94]. The authors reported that the adsorption mechanisms for Eu(III) included surface complexation and cation exchange, while the influence of principal ions naturally leached from clays as competitive factors for Eu retention. The authors utilized a 2-site non-electrostatic model to interpret surface complexation, achieving satisfactory data simulation. This involved considering the formation of monodentate surface complexes with Eu(III), $EuCO_3^+$, and $Eu(OH)_2^+$ at both strong and weak sites [94]. Lujanienė et al. [95] investigated the synthesis of composites using chitosan, natural clay such as montmorillonite and zeolite, along with cross-linking agents (epichlorohydrin, sodium tripolyphosphate, glutaraldehyde), and plasticizers (glycerol). Batch experiments were conducted to explore the adsorption behavior of cesium (Cs(I)), cobalt (Co(II)), and (Eu(III)) ions. The composites exhibited maximum adsorption capacities of 1400 mg/g for Cs(I), 900 mg/g for Co(II), and 18 mg/g for Eu(III) (Table 1). The adsorption data aligned more closely with the Langmuir isotherm model, suggesting favorable monolayer adsorption of Cs^+, Co^{2+}, and Eu^{3+} at homogeneous sites within the composites. Furthermore, the experimental results were better described by the pseudo-2nd order non-linear kinetic model for most elements and adsorbents [95]. Table 1 summarizes various NC and NC composites used to remove radionuclides from water.

A comparison of U(VI) adsorption performance among various adsorbents [91,96–104] reveals that NCs exhibit competitive capabilities (Fig. 4(b)). For instance, Jordanian Bentonite shows a maximum adsorption capacity of 62.12 mg/g [99], which is comparable to other materials like polyacrylamide (65.30 mg/g) [97] and coated Illite (54.35 mg/g) [91]. However, some advanced materials such as Citrate·Mg–Al LDH demonstrate significantly higher capacities (180.00 mg/g) [103], indicating superior performance (Fig. 4(b)). Meanwhile, immobilizing nZVI and Wool-AO@ZnO also outperform NCs with capacities of 107.80 mg/g [104] and 95.60 mg/g [96], respectively. Despite these differences, the adsorption capacities of NCs remain favorable when compared to common alternatives such as Amberjet resin (37.30 mg/g) [100] and polyurethane foam (26.30 mg/g) [98], making them a viable option for U(VI) removal in certain applications.

5.3. Dyes

The pervasive issue of dye contamination in water sources has spurred intensive research into effective remediation strategies, focusing on the adsorption capabilities of NC. Dyes, ubiquitous in various industries, including textiles, printing, and manufacturing, often find their way into water bodies, leading to aesthetically displeasing water and posing potential risks to aquatic life and human health [105]. NCs exhibit a notable capacity for adsorbing dye molecules from aqueous solutions owing to their surface reactivity, porous structure, and high surface area.

Salam et al. [106] used the modified hydrophilic bentonite NC to assess the sorptive removal of Orange G dye (OG dye) from aqueous solutions (synthetic and real water samples). The results demonstrated the rapid removal of OG dye by the obtained NC within 60 min, exhibiting an adsorption capacity of 39.40 mg/g. Furthermore, the findings substantiated the suitability of employing the pseudo-2nd order kinetic model to characterize the sorption process. Moreover, the spontaneous nature of the adsorption, coupled with its endothermic nature, was confirmed, with a positive entropy change. Furthermore, the authors evaluated the potential of utilizing the synthesized NC for OG dye adsorption using six distinct real water samples sourced from varying origins, showcasing the notably high efficacy of the obtained NC in a diverse aquatic environment [106]. On the other hand, the removal of two cationic dyes (Basic Green 4 (BG4) and Basic Yellow 28 (BY28)) using chemically modified montmorillonite NC was investigated through central composite design [107]. The results demonstrated a strong concordance between the predicted values derived from the model and the experimental outcomes for both BG4 (R^2 = 0.96) and BY28 (R^2 = 0.93). The central composite design proposed optimum conditions (pH 10, 52–60 min, and 0.45 g/L) to achieve maximal dye removal via the adsorption process. At these optimal conditions, the removal efficiencies reached 82.35 % for BG4 and 98.78 % for BY28, respectively [107]. Other researchers developed a novel nanohybrid NC composite (magnetic chitosan-salicylaldehyde/NC (MCH-SAL/NCLA)) for the removal of azo dye, acid red 88 (AR88), from simulated wastewater [108]. The authors combined RSM with Box-Behnken design (BBD) to optimize the adsorption process, conducting 29 experiments to explore the impact of various adsorption variables. The experimental data unveiled the optimal conditions for AR88 removal, achieving an impressive 75.16 % removal efficiency at optimum conditions (NCLA loading at 41.80 %, a dosage of 0.6 g/L, pH 4, and 86.17 min). The sorption of AR88 onto MCH-SAL/NCLA showed adherence to pseudo-1st order and Temkin models, with a remarkable maximum adsorption capacity of 173.5 mg/g [108]. Far et al. [109] reported a remarkably efficient organic dye removal via the innovation of the NC-MOF composite [109]. This unique composite was meticulously crafted through an in-situ solvothermal synthesis, fostering the growth of Cr-MOF directly onto the NC structure. The obtained composite exhibited superior specific surface area (4959 m^2/g) and enhanced sorption capacity as 200.24, 214.23, 207.56, and 213.16 mg/g for Acid Blue 92, Direct Red 31, Methyl Orange (MO) and Methylene Blue (MB), respectively [109] (Table 2). Furthermore, Marandi et al. [110] reported the preparation of super adsorbent poly (acrylamide-*co*-itaconic acid)/laponite NC hydrogels (NCHs) [110], and the synthesis process was achieved through in situ free-radical polymerization of acrylamide and itaconic acid within an aqueous medium, utilizing NC as a crosslinker. In the subsequent adsorption studies, the observed rates of dye uptake by the NCHs exhibited a consistent order (Table 2): methylene green (MG) > MB > crystal violet (CV) [110].

Fig. 4(c) shows a comparison of methylene blue adsorption capacities among various adsorbents, highlights the performance of NCs relative to other materials [109,111–119]. Nanoclay-MOF exhibits a significant adsorption capacity of 213.16 mg/g [109], demonstrating its efficiency compared to traditional adsorbents such as activated carbon (81.20 mg/g) [118] and acid modified lignin (83.20 mg/g) [112].

Table 2
Nanoclay and nanoclay composites for the removal of dyes from aqueous solution.

Adsorbents	Targeted Pollutants	Sorption capacity (mg/g)	Optimum conditions				Followed theoretical models
			Concentration (mg/L)	pH	Contact time (min)	Dosage (g/L)	
NC-MOF [109]	Acid Blue 92	200.24	30.0–150.0	5.0	30	0.2	Pseudo-second-order, Langmuir
Natural NC [206]	Crystal violet	206.73	20.0–500.0	7.0	120	0.6	Pseudo-second-order, Freundlich
Functionalized biochar-clay nanocomposite [123]	Crystal violet	281.24	5.0–200.0	6.0	120	0.4	Pseudo-second-order, Freundlich
Na-Montmorillonite NC [207]	Crystal violet	5.81[a]	0.98–3.67[a]	11.0	120	0.4	Pseudo-second-order, Langmuir
Modified Montmorillonite NC [208]	Crystal violet	196.08	10.0–50.0	4.0	120	2.5	Schott's second order, Langmuir
Hydrogel-clay nanocomposite [209]	Brilliant Cresyl Blue	494.20	40.0–500.0	6.0	90	0.5	Pseudo-second-order, Langmuir
Chitosan/Ag-hydroxyapatite nanocomposite [201]	Rhodamine B	127.61	0.5–20.0	7.0	120	0.5	Pseudo-second-order, Langmuir
Cellulose-derived carbon/montmorillonite nanocomposites [210]	Methylene blue	138.10	60.0–160.0	8.0	240	1.0	Pseudo-second-order, Redlich-Peterson
NC-MOF [109]	Methylene blue	213.16	30.0–150.0	5.0	30	0.2	Pseudo-second-order, Langmuir
PVA/CMC/halloysite NC [211]	Methylene blue	40.60	10.0–110.0	10.0	240	1.2	Pseudo-second-order, Freundlich
Cellulose–Clay Nanocomposite Hydrogels [113]	Methylene blue	782.90	10.0–200.0	6.0	2400	62.5	Pseudo-second-order, Langmuir
Nanocellulose-clay film [212]	Methylene blue	127.64	5.0–150.0	6.0	240	0.4	Pseudo-second-order, Sips
Halloysite NC [159]	Methylene blue	27.18	10.0–150.0	6.2	30	2.0	Pseudo-second-order, Langmuir
Hydrophilic bentonite NnC [106]	Orange G	39.40	25.0–150.0	8.0	120	1.0	Pseudo-second-order, intra-particle diffusion
Na-Montmorillonite NC [207]	Toluidine Blue	5.24[a]	1.30–4.90[a]	11.0	120	0.4	Pseudo-second-order, Langmuir
Hydrogel-clay nanocomposite [209]	Safranine-T	484.20	40.0–500.0	6.0	90	0.5	Pseudo-second-order, Langmuir
NC-MOF [109]	Methyl orange	207.56	30.0–150.0	5.0	30	0.2	Pseudo-second-order, Langmuir
Modified Montmorillonite NC [208]	Sunset yellow	175.44	10.0–50.0	4.0	120	2.5	Schott's second order, Langmuir
NC-MOF [109]	Direct Red 31	214.23	30.0–150.0	5.0	30	0.2	Pseudo-second-order, Langmuir
Modified Montmorillonite NC [208]	Naphthol green	263.161	10.0–50.0	4.0	120	2.5	Schott's second order, Langmuir

[a] mmol/g.

However, clay nanocomposite hydrogels show an exceptional adsorption capacity of 782.90 mg/g [113], surpassing other materials, including magnetic biochar (163.00 mg/g) [115] and lignin-steel sludge composite (153.92 mg/g) [114] (Fig. 4(c)). Lower-performing adsorbents such as Marula seed husk (33.00 mg/g) [111] and Lemongrass biowaste (43.16 mg/g) [116], underscore the superior performance of NC-based materials in Methylene blue adsorption. While some alternatives such as bagasse biochar (161.00 mg/g) [117] and oxone-treated hydrochar (86.70 mg/g) [119] also offer competitive capacities (Fig. 4(c)), NCs remain a potent option in dye removal applications, particularly when combined with metal-organic frameworks (MOFs).

5.4. Emerging pollutants

Emerging pollutants, a category encompassing diverse contaminants, include pharmaceuticals, pesticides, and various other chemicals, often not typically monitored in water systems [120]. These compounds pose a significant challenge in water quality management due to their potential long-term impacts on environmental and human health. Their presence in water sources, primarily originating from industrial, agricultural, and domestic sources, raises concerns regarding their persistence, bioaccumulation, and potential adverse effects even at trace concentrations [121]. However, NC has garnered attention for its potential in adsorbing these emerging pollutants, owing to its unique surface characteristics, high surface area, and tunable properties. In this regard, the bentonite NC was investigated in a batch system for the sorption/desorption of vancomycin antibiotic from aqueous solution [122]. The study findings revealed a pronounced pH dependency in both processes. Optimal adsorption occurred under acidic conditions, while desorption peaked in alkaline environments (Table 3). Additionally, the presence of Na^{+}, Ca^{2+}, and Al^{3+} in the solution notably improved vancomycin desorption from the bentonite surface. The superior desorption performance was found in the following order: $Al^{3+} > Ca^{2+} > Na^{+} > H_2O$ [122]. Furthermore, the bentonite NC exhibited a Langmuir sorption capacity of 370.37 mg/g for vancomycin and followed pseudo-2nd order kinetic model.

Moreover, a functionalized algal biochar-nano clay composite was synthesized using batch and continuous flow systems for norfloxacin antibiotic removal from water [123]. The obtained nanocomposite exhibited a remarkable maximum sorption capacity of 192.80 mg/g for norfloxacin via the Langmuir model. The excellent fit of the experimental data to both Clark and Freundlich models indicated the likelihood of multi-layer sorption of norfloxacin molecules. In continuous flow mode, the nanocomposite showcased a notable maximum bed capacity of 37.90 mg/g for norfloxacin. Applying theoretical models further suggested a cooperative heterogeneous sorption process [123]. Another study reported the sorption of pharmaceutical compounds (diclofenac, naproxen, gemfibrozil, and ibuprofen) from aqueous solutions, employing magnetic nanoparticles coated zeolite (MNCZ) [124]. Notably, the removal process favored lower pH values, where the

Table 3
Nanoclay and nanoclay composites for the removal of emerging pollutants from aqueous solution.

Adsorbents	Targeted Pollutants	Sorption capacity (mg/g)	Optimum conditions				Followed theoretical models
			Concentration (mg/L)	pH	Contact time (min)	Dosage (g/L)	
Iron coated polymer clay nanocomposite [213]	Ciprofloxacin	39.06	0.5–40.0	7.0	240	1.0	Pseudo-second-order, Freundlich
Nanocomposite polyelectrolytes [130]	Ciprofloxacin	58.60	5.0–200.0	9.0	30	0.3	Pseudo-first-order, Langmuir
Kaolin-alginate Beads [214]	Ciprofloxacin	68.36	20.0–140.0	4.0	1440	0.8	Pseudo-first-order, Langmuir, Temkin
Halloysite NC [159]	Enrofloxacin	33.57	10.0–150.0	6.2	30	2.0	Pseudo-second-order, Langmuir
Functionalized biochar-clay nanocomposite [123]	Norfloxacin	192.80	5.0–150.0	6.0	120	0.4	Pseudo-second-order, Freundlich
Nanocellulose-clay film [212]	Norfloxacin	101.68	5.0–150.0	6.0	240	0.4	Pseudo-second-order, Sips
Smectite clay-zirconium oxides NC [215]	levofloxacin	356.98	10.0–200.0	5.5	90	0.1	Pseudo-second-order, Sips
Bentonite NC [122]	Vancomycin	370.37	25.0–175.0	4.0	30	0.4	Pseudo-second-order, Langmuir
Iron coated polymer clay nanocomposite [213]	Gemfibrozil	24.79	0.5–40.0	4.0	300	1.0	Pseudo-second-order, Freundlich
Montmorillonite NC [55]	Ibuprofen	95 %	10.0–800.0	6.0	1440	15	Freundlich
β-cyclodextrin modified Cloisite 15A nanoclay composite [216]	Ibuprofen	1.10	3.0–10.0	6.0	120	0.1	Elovich, Temkin and Langmuir
Nanocomposite polyelectrolytes [130]	Tetracycline	291.70	5.0–200.0	11.0	30	0.3	Pseudo-first-order, Langmuir
Halloysite NC [59]	Oxytetracycline	52.4	10.0–500.0	4.75	720	1.0	Pseudo-second-order, Hill
Bentonite NC [152]	p-nitrophenol	284.25	10.0–600.0	5.0	20	2.0	Pseudo-second-order, Langmuir
Chitosan/bentonite nanocomposites [217]	Tartrazine	294.10	20.0–300.0	2.5	80	0.2	Pseudo-second-order, Langmuir
Iron coated polymer clay nanocomposite [213]	Atenolol	15.63	0.5–40.0	10.0	180	1.0	Pseudo-second-order, Freundlich
Nanocomposite polyelectrolytes [130]	Amoxicillin	97.60	5.0–200.0	11.0	30	0.2	Pseudo-first-order, Langmuir
Montmorillonite NC [55]	Paracetamol	63–67 %	10.0–800.0	6.0	1440	15	Freundlich
Montmorillonite NC [55]	Carbamazepine	97 %	10.0–800.0	6.0	1440	15	Freundlich

compounds exhibited more efficient removal. However, their removal efficiency decreased as the pH shifted towards more basic conditions. The initial concentration seemed to have minimal impact on the removal efficiency at lower concentrations, but as concentrations increased, particularly for ibuprofen, the removal efficiency notably decreased [124]. Diclofenac's removal, however, appeared independent of time, while naproxen, gemfibrozil, and ibuprofen removal were notably influenced by contact time, achieving up to a 95 % removal within 10 min using MNCZ. The adsorption of these pharmaceutical compounds onto MNCZ revealed the best fit to the Freundlich isotherm model and pseudo-2nd order kinetic model. Moreover, the authors used MNCZ in column adsorption studies, showing significantly higher removal efficiency (>99 %) compared to these alternative methods used in drinking water treatment plants [124].

Furthermore, NC significantly plays an essential role in mitigating the presence of pesticides in water sources, thereby addressing concerns regarding their potential persistence, bioaccumulation, and associated ecological and health risks [125]. Pesticides, synthetic chemical substances used extensively in agriculture to control pests and enhance crop yields, have become a significant concern as water contaminants due to their potential adverse impacts on the environment and human health [126,127]. These chemicals enter water sources through various pathways, such as surface runoff and leaching from agricultural fields, posing contamination risks to aquatic ecosystems and drinking water supplies. NC has emerged as a promising solution for mitigating pesticide pollution in water. Their high surface area, porous structure, and surface reactivity facilitate the adsorption of pesticide molecules from water, effectively reducing their concentrations. A study explored the efficacy of combining coagulation and adsorption for removing multiple pesticides [128]. The study assessed their performance using various NCs, including nano bentonite and montmorillonite (organically modified). Adsorption using organically modified nano-montmorillonite revealed removal efficiencies between 60.10 and 77.00 % for different pesticides, while nano-bentonite displayed removal efficiencies varying from 51.70 to 69.30 %. Additionally, the study investigated the sorption efficiency in combination with coagulation. Moreover, the removal efficiencies ranged from 75.10 % for pendimethalin to 96.30 % for atrazine when using alum in conjunction with nano-bentonite, yielding an overall removal efficiency of 87.80 %. In comparison, when alum was combined with halloysite NC, the removal efficiencies varied from 71.10 % for pendimethalin to 92.50 % for cypermethrin, with a total removal efficiency of 80.70 % [128]. Other researchers delved into using surfactant-modified pillared montmorillonites for bentazon removal from aquatic medium [129]. The obtained sorbent was synthesized through an intercalation process involving cetyltrimethylammonium bromide and montmorillonite. The authors examined several factors to optimize the adsorption process (pH = 3, NC = 0.5 g/L, and 20 mg/L of $[Bentazon]_0$). Their findings highlighted a rapid initial adsorption phase followed by a gradual slowdown (equilibrium ≈ 90 min). Additionally, the authors explored the impact of pH on adsorption capacity. Their results showcased a significant influence: as pH levels increased from 3 to 11, the removal efficiency decreased notably, from 99 % at pH 3 to 35 % at pH 11 [129].

The adsorption performance of NCs for tetracycline was compared to other adsorbents [130–139], revealing a competitive edge (Fig. 5(a)). Montmorillonite NC exhibited a relatively high adsorption capacity at 250.00 mg/g [136], which is close to the performance of leading materials such as Fe/Cu-GO and Zeolite Imidazole Frameworks with capacities of 302.50 mg/g [131] and 303.00 mg/g [135], respectively. Although nanocomposite polyelectrolytes demonstrated a slightly lower

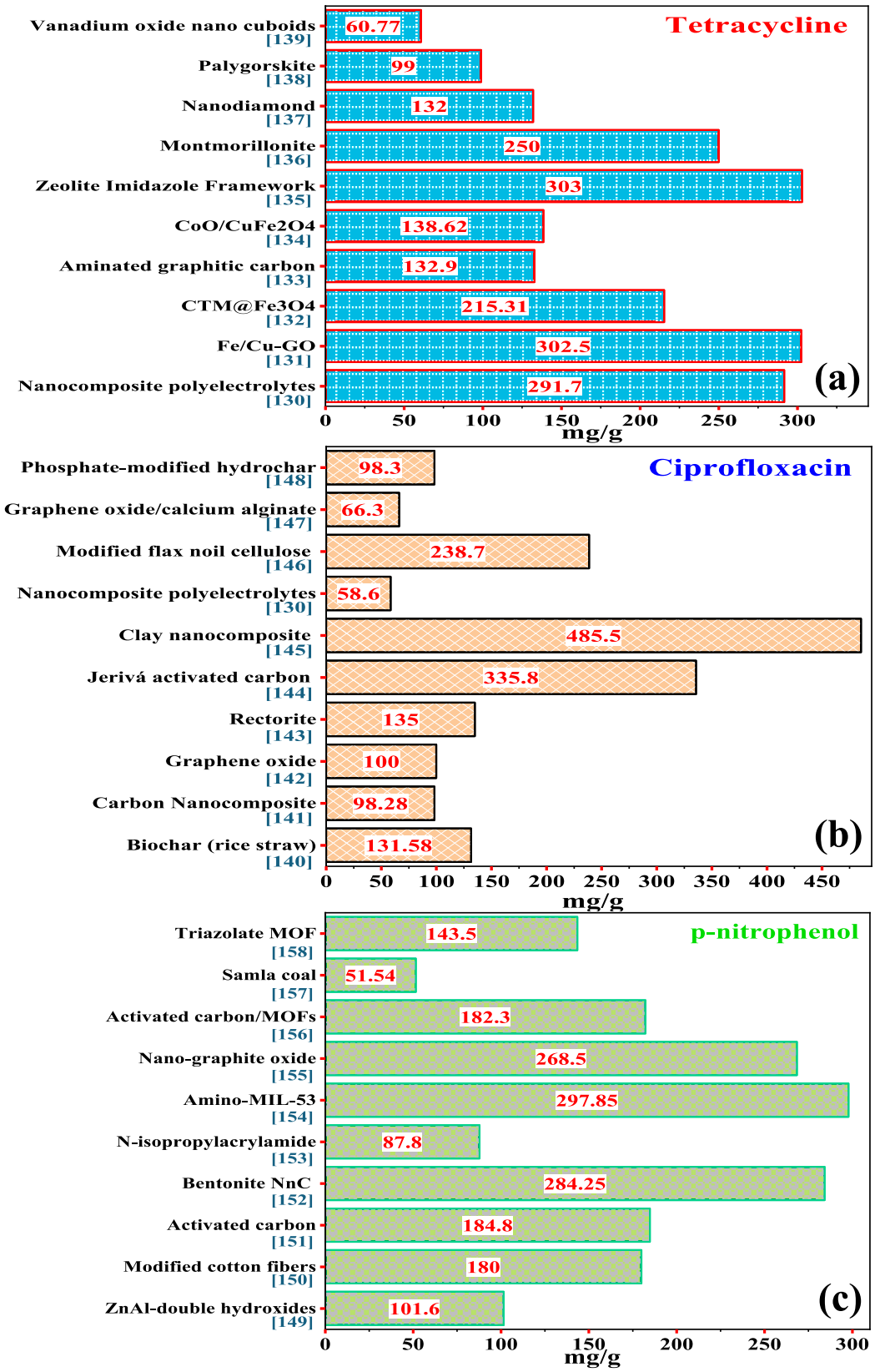

Fig. 5. Comparison of NC and other adsorbents for selective emerging pollutants removal (a) Tetracycline, (b) Ciprofloxacin, and (c) p-nitrophenol.

capacity of 291.70 mg/g [130], the performance of Montmorillonite is notably higher than that of other conventional adsorbents such as aminated graphitic carbon (132.90 mg/g) [133] and $CoO/CuFe_2O_4$ (138.62 mg/g) [134] (Fig. 5(a)). Palygorskite and vanadium oxide nano cuboids exhibited much lower capacities of 99.00 mg/g [138] and 60.77 mg/g [139], respectively, highlighting the superior performance of Montmorillonite for tetracycline removal. Similarly, the performance of NCs for ciprofloxacin adsorption was also competitive when

compared to other adsorbents [130,140–148]. Clay nanocomposites displayed a remarkably high adsorption capacity of 485.50 mg/g [145], surpassing all other materials listed (Fig. 5(b)), including Jerivá activated carbon (335.80 mg/g) [144] and modified flax noil cellulose (238.70 mg/g) [146]. This impressive performance underscores the potential of clay nanocomposites in applications where high adsorption capacities are critical. In contrast, other adsorbents, such as graphene oxide (100.00 mg/g) [142], carbon nanocomposites (98.28 mg/g) [141], and phosphate-modified hydrochar (98.30 mg/g) [148], showed significantly lower adsorption capacities (Fig. 5(b)). These comparisons illustrate that NCs, particularly clay nanocomposites, offer substantial advantages in removing antibiotics like tetracycline and ciprofloxacin, making them promising candidates for advanced water treatment applications.

Fig. 5(c) demonstrates the adsorption performance of p-nitrophenol varies significantly across varied adsorbents materials [149–158]. Bentonite nanocomposite exhibited a high adsorption capacity of 284.25 mg/g [152], close to the capacity amino-MIL-53 with an adsorption capacity of 297.85 mg/g [154]. This places bentonite NnC among the top-performing materials (Fig. 5(c)), surpassing traditional adsorbents like activated carbon, which has an adsorption capacity of 184.80 mg/g [151]. Similarly, nano-graphite oxide also demonstrated a high adsorption capacity of 268.5 mg/g [155], however, still lower than that of bentonite NC. Other materials such as modified cotton fibers and activated carbon/MOFs showed moderate adsorption capacities of 180.00 mg/g [150] and 182.3 mg/g [156], respectively (Fig. 5(c)), while ZnAl-layered double hydroxides and triazolate MOF exhibited lower capacities of 101.60 mg/g [149] and 143.5 mg/g [158], respectively. N-isopropylacrylamide and samla coal displayed significantly lower adsorption capacities at the lower end of the spectrum, with values of 87.80 mg/g [153] and 51.54 mg/g [157], respectively. This comparison highlights the superior adsorption efficiency of bentonite NC composites for p-nitrophenol, underscoring their potential as highly effective materials for removing this pollutant from water.

5.5. Simultaneous adsorption of pollutants

NC's simultaneous adsorption of various pollutants represents a pioneering approach to water remediation strategies. The NC multifunctionality effectively targets a spectrum of contaminants, ranging from heavy metals and organic compounds to emerging pollutants. The unique surface characteristics of NCs provide numerous active sites, facilitating the concurrent adsorption of different contaminants in a single treatment process. Understanding and optimizing the simultaneous adsorption potential of NC for diverse pollutants holds promise for developing comprehensive and efficient water remediation systems.

Giannoulia et al. [159] reported halloysite NC for simultaneous and individual elimination of antibiotic enrofloxacin and MB dye from water [159]. Additionally, the study explored the regeneration of halloysite NC using cold-atmospheric plasma bubbling. The authors also reported that the calculated ratio for enrofloxacin was less than one in the binary system, signifying a decrease in its sorption capacity due to the presence of MB. Conversely, the ratio for MB slightly exceeded 1, suggesting either a synergistic effect or indicating that its adsorption capacity in the binary system is either boosted or unaffected by the presence of enrofloxacin. This observation may be ascribed to the elevated negative charge on the external surface of halloysite NC, leading to enhanced MB adsorption owing to its stronger cationic nature compared to enrofloxacin under the investigated pH conditions of the solution [159]. Moreover, Sorkhabi et al. [160] stated that the utilization of locally modified nano-clay to remove Cr(III) and acid brown dye is simultaneously present in model tannery wastewaters [160]. Results revealed that the maximum sorption values, achieved under optimized conditions (pH 4, 100 mg/L of each contaminant, 15 g/L of NC, and 3 min interaction time for Cr(III) and 30 min for the dye) reached 193.14 mg/g (Cr (III)) and 144.18 mg/g (dye) (Table 4). The study confirmed the synergistic and antagonistic adsorption in binary solutions. Kinetic modeling indicated adherence to the pseudo-2nd order model for simultaneous adsorption and followed Langmuir and Dubinin–Radushkevich isotherms for Cr(III), while dye adsorption followed

Table 4
Comparison of the simultaneous adsorption of various pollutants using nanoclay and nanoclay composites.

Adsorbents	Modifier	Solution matrix	Sorption capacity (mg/g)	Optimum conditions					Followed theoretical models
				pH	Contact time (min)	C_0 (mg/L)	Dosage (g/L)	Temp. (°C)	
Urmia NC [160]	CHPTAC	Cr(III)	193.14	4.0	30	100	15.0	15	Langmuir, Pseudo-second order
		Acid brown	144.18			100			Redlich–Peterson, Pseudo-second order
Organo-montmorillonite NC [218]	HDTMA and Z16 surfactants	Cu(II)	14.12	5.0	30	60	5.0	25	Langmuir, Pseudo-second order
		phenol	3.75			150			Langmuir, Pseudo-second order
Natural red NC [219]	HDTMA	Cr (VI)	0.086[a]	5.5	360	0.2[b]	4.0	25	Langmuir–Freundlich, Pseudo-first order
		phenol	0.012[a]			0.6[b]			Dual site Langmuir–Freundlich, Pseudo-first order
Montmorillonite NC [220]	Dodecyl sulfobetaine	Cu(II)	9.5	5.0	30	15	1.0	NR[c]	NR[c]
		MB	150.2			250			
Dual-cation organomontmorillonite [221]	CSH, TTAC, CTAC, STAC	Zn(II)	100 %	11.0	10	40	1.0	50	Freundlich
		phenol	65.5 %			40			
Amphoteric montmorillonite NC [222]	Octadecane-betaine	Bisphenol	80.77	4.0	1440	10	2.0	30	Langmuir, Pseudo-second order
		Cd(II)	42.11			40			Freundlich, Pseudo-second order
Halloysite NC [159]	–	MB	20.20	6.5	60	40	2.0	28	Pseudo-second order
		Enrofloxacin	13.64			40			Pseudo-second order

[a] mmol/g.
[b] mmol/dm^3.
[c] NR = not reported.

the Redlich–Peterson isotherm in both scenarios. Thermodynamic analysis revealed the spontaneous nature of Cr(III) adsorption and the non-spontaneous nature of dye adsorption, with Cr(III) adsorption being exothermic and dye adsorption being endothermic. Furthermore, entropy decreased during the adsorption of both contaminants. The RSM results suggested that increasing the concentration of Cr(III) and dye independently elevated their respective adsorption capacities while exerting a negligible effect on the adsorption of the other contaminant [160].

5.6. Sorption mechanisms

The adsorption process at the surface of NC minerals is closely related to the charge chemistry of the clay surface, which dictates how pollutants interact with it. Several mechanisms have been identified for the sorption of metal ions by NC, including physical adsorption, micro-precipitation, ion exchange, and chemisorption [161] (Fig. 6). Physical adsorption occurs due to van der Waals forces, where metal ions are attracted to the surface of the clay without forming a strong chemical bond. Micro-precipitation involves the exchange of metal ions at permanently charged sites on the clay surface, forming stable metal complexes, particularly at edge sites rich in hydroxyl groups. Chemisorption is a stronger interaction where metal ions form covalent bonds with the clay surface, often forming metal-organic complexes. Additionally, the formation of organoclay can be achieved by exchanging native cations with organic molecules, enhancing the clay's ability to adsorb a broader range of contaminants [162]. These mechanisms highlight the versatility of NC minerals in adsorbing various metal ions, making them highly effective in water remediation applications.

The adsorption mechanisms of various pollutants by NCs are a complex process influenced by multiple factors and interactions between the pollutant molecules and NCs surface and interlayer structure. Generally, the adsorption onto NCs for heavy metals primarily involves surface complexation and ion exchange (Fig. 6). The high surface area and negatively charged sites on NCs facilitate the attraction and binding of positively charged heavy metal ions, allowing them to form stable surface complexes. Additionally, ion exchange occurs as these metal ions replace exchangeable cations on the NCs surface [163]. The layered structure of NCs offers interlayer spacing and edges that further contribute to the adsorption process. Zhang et al. [65] reported that increasing the solution pH increases the electronegativity of NCs adsorbents, primarily attributed to the deprotonation of diverse functional groups at higher pH values. This elevated electronegativity facilitates the attraction of more contaminants onto the adsorbents and renders the desorption of adsorbed heavy metal ions. Due to the isomorphism substitution, most NCs (i.e., montmorillonite, kaolinite, halloysite) possess a permanent negative charge on the surface. This charge is balanced by exchangeable cations. The cationic heavy metal ions can replace the adsorbed exchangeable cations. This characteristic positions NCs as prominent products in adsorbents, with ion exchange playing a key role in contaminant removal (Fig. 6). Moreover, there's ion exchange occurring between pollutants and protons in functional groups like –COOH or –OH introduced by incorporated organic or inorganic modifiers. The sorption mechanism of heavy metals onto alginate/clay can be ascribed to the presence of –OH groups on the NC [164]. The involvement of hydroxyl groups in the reaction with acrylic acid results in the generation of ester bonds. These reactions culminate in the synthesis of poly(acrylic acid) grafted onto alginate/clay, ultimately yielding a composite of poly(acrylic acid) integrated with clay and alginate. The verification of this mechanism is substantiated by the presence of absorption bands at 1771 cm^{-1}, 1642 cm^{-1}, 1471 cm^{-1}, and 1423 cm^{-1} in the FTIR spectrum of alginate/clay-g-poly(acrylic acid) ink [164].

Shaik et al. [165] investigated the adsorption of Ethidium Bromide (EB) onto Pyrophyllite NC (PNC) for the first time. The study highlighted that at a pH above the point of zero charge (PZC) of PNC and considering the pKa values of protonated EB, a substantial coulombic interaction occurs between the positively charged EB molecules and the negatively charged PNC surface. Computational studies further supported the hypothesis that surface-adsorbed solvent molecules are replaced, leading to stronger irreversible adsorbate-adsorbent interactions through hydrogen bonding and hydrophobic forces [165]. Moreover, Sirvi et al. [15] investigated the Cs sorption performance of three clay geosorbents sampled from different regions of Gujarat, India, focusing on the impact of clay structure and the presence of organic contaminants. The study identified ion exchange as the predominant mechanism for Cs uptake, attributed to isomorphic substitution within the clay's structural

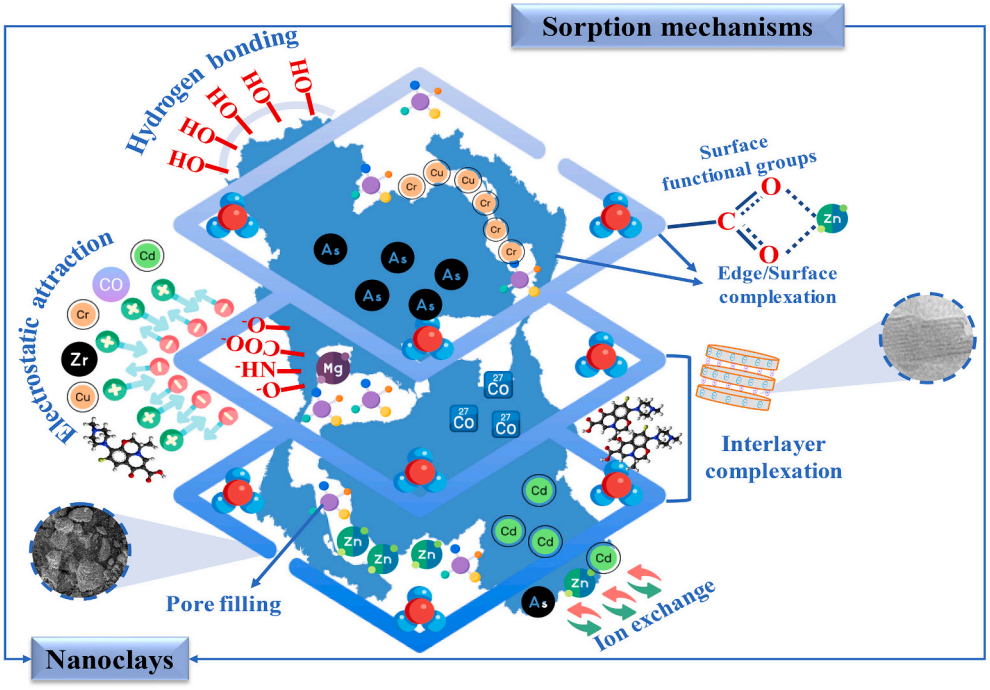

Fig. 6. Possible sorption mechanism of various pollutants onto nanoclays.

framework. The formation of outer sphere complexes was noted, driven by electrostatic interactions between hydrated Cs^+ ions and negatively charged surfaces at basal, interlayer, or edge sites. Additionally, the study found that inner sphere complexes could form through electrostatic or covalent interactions between surface-active sites and partially or fully dehydrated Cs^+ ions, particularly in interlayer regions where isomorphic substitution occurs in the tetrahedral sheets [15].

In the case of dyes, the adsorption onto NC is commonly governed by electrostatic interactions, van der Waals forces, and specific interactions between the dye molecules and the NC surface. The dyes are typically attracted to the charged sites on the NC, leading to their binding and removal from the aqueous solution. Hassani et al. [107] investigated the sorption mechanism of two cationic textile dyes (Basic Yellow 28 and Basic Green 4) onto NC [107]. NC particles subjected to chemical modification exhibited a negative surface charge at the ambient pH (−15.8 mV) [107]. This is attributed to the presence of negatively charged functional groups, namely Si—O and Al—O groups [107]. The process entails electrostatic interactions occurring between the negatively charged functional entities located on the surface of the modified NC and ions originating from the dye molecules. An additional mechanism involves the creation of hydrogen bonds between the Si-OH, Al-OH, and N—H groups present in the adsorbent, and the oxygen and nitrogen-containing groups found in the dye molecules (Fig. 6). Additionally, hydrophobic interactions between the long-chain alkyl groups of the modified NC and the dye molecules were also contributed to the sorption of these dyes [107]. Moreover, Salam et al. [106] observed that the interaction between the OG dye and the ODA-NC was electrostatic in nature, with a substantial dependence on the solution's pH [106]. Zhang et al. [166] reported the development and application of montmorillonite (MMT) modified with chitosan for the adsorption of methylene blue (MB) dye under varying pH conditions. Through molecular dynamics simulations, the authors found that pure MMT facilitates monolayer adsorption, while the chitosan-modified MMT (CMMT) supports multilayer adsorption [166]. Electrostatic attraction, intermolecular π–π interactions, and hydrogen bonding drive the adsorption mechanisms. The study also revealed that the adsorption efficiency of CMMT increases with pH, reaching a peak efficiency of 80 % at pH 9.5, although higher pH levels reduce the composite's stability.

For pharmaceutical compounds, pesticides, and other organic pollutants, the adsorption mechanism involves a combination of interactions, such as hydrogen bonding, π-π interactions, hydrophobic interactions, and electrostatic forces [55]. These pollutants possess diverse molecular structures and properties influencing their adsorption behavior on the NC surface. The hydrophobic domains on the NC surface can attract and interact with the non-polar regions of organic compounds, while polar functional groups may engage in hydrogen bonding or electrostatic interactions with the charged sites of the NC. Authors reported that the cationic form of oxytetracycline (OTC) forms complexes with the negatively charged halloysite NC (HNC) via electrostatic interaction [59]. As the pH surpasses 3.5, electrostatic complexation between the cationic dimethylamine species of OTC and the anionic surface of HNC becomes prominent during the adsorption process [59]. Moreover, at low pH conditions, an observable increase in the final pH suggests ion exchange, indicating potential interactions with hydroxide ligands on the surface. Beyond pH 7.5, electrostatic repulsion diminishes OTC-HNC interaction due to the negatively charged surfaces of both entities. Furthermore, the presence of positively charged Al_2O_3 groups and negatively charged SiO_2 groups in both the inner and outer lumens of HNC facilitates the chemisorption process with tricarbonylamide and dimethylamine in the zwitterionic form of OTC [59]. Within the pH range of 2.5–8.0, specific adsorption is indicated by the potential formation of a robust covalent bond through monolayer-complexation of OTC with the surface, with no involvement of intervening water molecules. Time-dependent OTC adsorption suggests a chemisorption mechanism. The modeling of isotherm data suggests a cooperative adsorption phenomenon, with OTC binding to different surface sites of halloysite [59]. Furthermore, the selectivity of NCs towards different pollutants is often governed by the pollutants' specific surface characteristics, functional groups, and physicochemical properties. Parameters such as contaminant size, charge, solution pH, and ionic strength significantly influence both the efficiency and mechanism of NC adsorption.

6. Regeneration of spent nanoclays

Regeneration of spent NC adsorbents is critical to their lifecycle, ensuring the continuous and sustainable removal of various pollutants from water sources. Regeneration, defined as the recycling or recovery of spent adsorbents using technically and economically feasible methods, holds immense importance in pollution control, where cost-effectiveness is paramount. Various regeneration methods have been explored to retain the adsorption capacity of NC adsorbents, including thermal regeneration, steam regeneration, pressure swing regeneration, vacuum regeneration, microwave regeneration, ultrasound regeneration, chemical regeneration, oxidative regeneration, ozone regeneration, and bio-regeneration. These methods can be employed individually or in combination, such as thermochemical regeneration or electrochemical regeneration, to optimize the regeneration process. This section examines the regeneration processes for spent NCs, emphasizing their role in restoring adsorption capacity and ensuring sustainable reuse. It discusses prevalent regeneration methods such as thermal regeneration, chemical regeneration, and biological degradation, highlighting their effectiveness and practical applications in water treatment.

6.1. Thermal regeneration

Thermal regeneration stands as a prominent method for restoring the adsorption capacity of spent NC adsorbents. In this process, the spent adsorbents are subjected to elevated temperatures to desorb and remove the adsorbed contaminants. Thermal regeneration exploits the desorption of pollutants by applying heat, which facilitates the release of contaminants from the adsorbent surface. The desorbed pollutants are then collected or treated separately while the regenerated NC adsorbents regain their adsorption capacity. The effectiveness of thermal regeneration depends on various factors, such as the nature of the adsorbate, the temperature and duration of heating, and the characteristics of the NC adsorbent. High temperatures are typically employed to ensure efficient desorption, although care must be taken to avoid thermal degradation of the adsorbent material. The thermal regeneration process typically involves heating the NC particles to a specific temperature, ranging from 25 to 950 °C, depending on the type of NC and the desired outcome. Thermal regeneration offers several advantages, including simplicity, cost-effectiveness, and the ability to regenerate adsorbents for multiple cycles. However, it may not be suitable for adsorbents sensitive to high temperatures or adsorbates with high thermal stability [167–170].

Zhu et al. [171] investigated the regenerability of acid-activated palygorskite (APalx) through in-situ desorption of toluene and recycling experiments. The authors reported that APal5 could be efficiently regenerated by thermal desorption at 100 °C with a N_2 gas flow rate of 50 mL/min [171]. The study demonstrated that APal5 maintained good reproducibility over six cycles of toluene adsorption, with a recycling efficiency exceeding 99 %. Analysis of the diffusion rate constants (k) and constant τ values indicated no significant changes in mass transfer and diffusion resistance of APal5, suggesting that its porous structure and surface properties remained effective for toluene adsorption [171].

Thermal and Fenton oxidation methods are utilized to regenerate exhausted zeolites. Sun et al. [172] regenerated zeolite through high-temperature heating (450, 550, and 650 °C), with optimal adsorption capacity (90–105 %) achieved at 450 °C [172]. However, heating at higher temperatures may compromise zeolite structure and decrease

adsorption capacity. Fenton oxidation, though effective, also damages the adsorbent surface and pores. Ferric ions in Fenton reagent diminish ion exchange capacity [173]. Alternatively, air calcination yielded slightly better results than Fenton oxidation [174]. Thermal regeneration is costly due to energy requirements and weight loss of adsorbent (5–15 %) after each cycle. Thus, alternative regeneration methods, such as photocatalytic and biological regeneration, are explored to maintain adsorbent integrity.

6.2. Chemical regeneration

Chemical regeneration is a key method for restoring the adsorption capacity of NC adsorbents, ensuring their continued effectiveness in water treatment applications. Generally, adsorption and desorption processes occur concurrently, maintaining a balance to some extent. However, by adjusting the solution environment, the dominance of desorption can be achieved, facilitating the regeneration of adsorbents. Acidic, alkaline, saline, and organic solutions are commonly employed as eluents for chemical regeneration. Acidic solutions, rich in H^+ ions, effectively replace contaminants on adsorption sites via ion exchange, making them particularly suitable for regenerating clay-based adsorbents. These adsorbents primarily adsorb contaminants through ion exchange processes. Similarly, salt solutions such as NaCl or KCl can facilitate regeneration by exchanging Na^+ or K^+ ions with contaminants. In contrast, organic solvents solvate organic contaminants from spent adsorbents, promoting their regeneration [65]. For instance, acetone solutions have been used to extract safranine dye from clay-based adsorbents [175]. The elution of methylene blue from composite adsorbents of clay and papaya seeds using an aqueous HNO_3 solution (0.01 to 0.1 M) exhibited a consistent 90 % desorption efficiency over five successive regeneration cycles [176]. However, Yang et al. [177] observed a reduction in the desorption efficacy of hexadecyltrimethylammonium (HDTMA)-modified montmorillonite (HMM) when using NaOH as the desorbing agent for phenol [177]. Furthermore, eluent desorption methods may suffer from low efficiency, necessitating multiple elution cycles to achieve optimal regeneration. Nonetheless, chemical regeneration remains a valuable strategy for regenerating NC adsorbents, contributing to their sustainable use in water treatment.

6.3. Biological degradation

Biological degradation or bioregeneration of NC adsorbents involves the use of microorganisms to break down and degrade adsorbed contaminants, thereby restoring the adsorption capacity of the material. This process harnesses the natural metabolic activities of microorganisms to remediate polluted water sources. Microorganisms such as bacteria, fungi, and algae can colonize the surface of NC adsorbents and utilize the adsorbed contaminants as a nutrient source. Through enzymatic reactions and metabolic pathways, these microorganisms can transform organic pollutants into harmless by-products such as carbon dioxide, water, and biomass. Yang et al. [177] investigated bioregeneration for clays or modified clays and found it more effective than chemical regeneration [177], particularly for hexadecyltrimethylammonium (HDTMA)-modified montmorillonite. *Pityrosporum* sp. yeast facilitated the regeneration process, leading to complete phenol degradation and restoration of sorption capacity after repeated regenerations [177]. However, microbial regeneration suffers from a slow rate, limiting its suitability for large-scale treatments. Additionally, not all adsorbents are conducive to microbial regeneration, as certain reagents like cationic surfactants used for adsorbent modification can be toxic to microbes [178].

7. Nanoclays application in real wastewater treatment

NCs play a pivotal role in real wastewater treatment due to their unique properties, such as high surface area, cation exchange capacity, and surface reactivity. However, the effectiveness of NC-based adsorbents in actual wastewater systems is influenced by several factors, distinct from controlled laboratory conditions using synthetic solutions. Therefore, understanding the interaction of NCs with real wastewater is essential for scaling up adsorption technologies and enhancing the performance of wastewater treatment systems. Real wastewater differs significantly from synthetic solutions used in laboratory experiments. It contains a complex mixture of organic and inorganic contaminants, including heavy metals, dyes, pharmaceuticals, pesticides, and various organic pollutants. Additionally, real wastewater has varying pH levels, ionic strength, and the presence of competing ions and natural organic matter, which can affect the adsorption capacity and efficiency of NC materials. Therefore, NC-based adsorption systems must be tested under real-world conditions to assess their true performance and robustness. To move from laboratory research to practical wastewater treatment applications, pilot-scale studies using real wastewater are essential. These studies help identify the operational challenges and optimize the system parameters for effective pollutant removal. Pilot-scale applications of NC-based adsorbents provide valuable insights into the scalability of the technology, including the regeneration and reuse of NCs, system integration, and cost-effectiveness. Various NCs were investigated for their potential in treating real wastewater, showing superior sorption performance [179–185].

Anggraini et al. [179] investigated the practical application of organo-modified montmorillonite (O-MMT) for real pharmaceutical wastewater treatment plant (local pharmaceutical and healthcare products manufacturer at Sidoarjo city, East Java). Batch adsorption experiments were performed at 303.15 K for 24 h using an adsorbent dose of 10 g/L [179]. Wastewater samples were randomly collected from five different points at a pharmaceutical plant in Sidoarjo, East Java. The primary contaminants were amoxicillin and ampicillin, with initial concentrations of 0.16 and 0.11 mmol/L, respectively, along with trace amounts of ciprofloxacin, chloramphenicol, and cefotaxime. The removal efficiencies for the antibiotics initially showed the highest removal for amoxicillin, followed by ampicillin, with a total removal of 68.20 %. However, a gradual decline in removal efficiency was observed across five regeneration cycles, culminating in a 49.50 % total removal [179]. In another study, adsorption experiments were conducted using bentonite (BENT) and cetyltrimethylammonium bromide-modified bentonite (CTAB-BENT) to remove ampicillin from both synthetic wastewater and wastewater from a pharmaceutical company [180]. In the case of real wastewater, the adsorption capacity for ampicillin was found to be 59.3 % compared to 89.9 % in synthetic wastewater for BENT. The adsorption capacity of CTAB-BENT also decreased in real wastewater (90.6 %) compared to synthetic wastewater (100 %) [180]. This reduction in adsorption capacity was attributed to the competitive adsorption of other substances present in the real wastewater, which impeded the removal efficiency of ampicillin [180]. Moreover, Kahkha et al. [181] utilized modified sodium montmorillonite NC to treat real urban wastewater from Zabol city [181]. The authors reported that all metal ions were completely removed closed to 100 % and all heavy metals' removal efficiency was over 94 % [181]. Another study on using stevensite NC for the adsorption of tetracyclines from real wastewater was conducted in batch mode and using a pressurized continuous system [182]. The findings demonstrated that continuous wastewater flow through a system containing stevensite effectively removed tetracyclines, indicating successful water purification through tetracyclines adsorption by the NC [182].

8. Economic feasibility of NCs

NC adsorbents are a promising and cost-effective solution for removing pollutants from wastewater. NC has unique characteristics that make it an efficient and low-cost adsorbent. It has a high specific surface area (up to 950 m^2/g), high cation exchange capacity (up to 150 meq/100 g), and can be easily synthesized [186]. For instance, the

maximum adsorption capacity of NC for Congo red dye ranged from 31.50 to 2435.70 mg/g, which showed that NCs can achieve a significantly high sorption capacity [186]. Therefore, the low cost of NCs and the relatively low cost of the adsorption technique (5.0–200 USD/m^3) [187], makes the NCs promising and cost-effective sorbents for eliminating pollutants from wastewater. Several studies have investigated the technical performance of nano-adsorbents in terms of adsorption capacity and kinetics. However, economic performance evaluation is rarely discussed in the literature. The cost estimation of NC adsorbents encompasses various factors, from raw material acquisition and synthesis to operational deployment and regulatory compliance. In the laboratory scale, the cost of NC adsorbents includes the costs of raw materials, transportation, chemicals, energy, and other expenses.

Compared to other adsorbents, NCs offer significant economic advantages due to their lower raw material costs, simpler synthesis processes, and widespread availability. Olusegun and Mohallem [188] synthesized a kaolinite-supported $CoFe_2O_4$ nanocomposite for the treatment of 1 L wastewater containing doxycycline and Congo red, with a reported net cost of 0.131 USD/0.667 g [188]. The synthesis process involves chemical treatments and does not require high temperatures or pressures, which further reduces operational expenses. Furthermore, other authors synthesized a zeolite adsorbent from industrial by-products such as slag and fly ash for the adsorption of salad oil, with a production cost of 3.36 USD/kg [189]. Moreover, a functionalized algal biochar-clay composite was developed for the adsorption of norfloxacin and crystal violet dye, costing 5.72 €/kg [123]. The synthesis of this composite involved combining biochar derived from algae with NC minerals, which enhanced the adsorbent's properties. Although the cost was higher than simple clay-based adsorbents, it remained significantly lower than many other adsorbent materials. Using biochar and clay minerals, a cheap and abundant material, ensures that the production remains economically viable. In contrast, Kang et al. [190] reported that the synthesis of graphene oxide for phenol adsorption costs approximately 6800 USD/kg [190]. Graphene oxide production is inherently expensive due to the high cost of precursor materials (like graphite) and the complexity of the chemical oxidation and exfoliation processes involved. Despite its excellent adsorption capabilities, the prohibitively high cost makes graphene oxide less feasible for large-scale water treatment applications compared to NCs.

The future economic trends for NCs in water treatment are promising due to several key factors. Firstly, the ongoing research and development aimed at enhancing the performance and efficiency of NCs through modifications and hybrid composite formations are expected to drive down costs further and improve their competitive edge in the market. Integrating NCs with other treatment technologies and developing green synthesis methods can also contribute to reducing production costs and enhancing sustainability. Additionally, as regulatory frameworks and environmental policies become more stringent, the demand for cost-effective and efficient water treatment solutions like NCs is expected to rise. The scalability of NCs applications, combined with their low cost and high efficiency in removing various pollutants, positions them as a key player in the future landscape of water treatment technologies. Therefore, the economic trends for NCs are anticipated to be favorable, driven by their cost-effectiveness, ongoing advancements in material science, and increasing demand for sustainable water treatment solutions.

9. Sustainability evaluation

9.1. Sustainability assessment

The literature reveals a significant gap in the sustainability assessment of NC adsorbents, with few studies comprehensively evaluating their environmental and economic impacts over their entire life cycle. Addressing this gap is crucial for understanding the true potential of NCs in water treatment applications, particularly as the demand for sustainable technologies continues to grow.

Sustainability assessment of NC adsorbents involves analyzing their environmental footprint, resource use, and potential health impacts throughout their life cycle. This includes the extraction of raw materials, production processes, application in water treatment, and eventual disposal or recycling of used NCs. Evaluating these factors can help identify the benefits and trade-offs associated with using NCs over other materials. NCs, derived from naturally abundant resources, present an inherently lower environmental impact compared to synthetic adsorbents. However, the energy-intensive processes required for their modification and activation, such as calcination and chemical treatment, could offset these benefits if not carefully managed.

9.2. Overview of nanoclays sustainability

NCs have emerged as a sustainable solution for water treatment, particularly in the adsorption of aquatic pollutants. Assessing the sustainability of NCs for water treatment entails a comprehensive examination of various environmental and economic factors. Therefore, the sustainability assessment encompasses several key aspects:

(i) NCs are abundant in nature and can be sourced sustainably from clay deposits worldwide. Their widespread availability reduces the reliance on finite resources, contributing to long-term sustainability in water treatment applications. Thus, this factor aligns with the aspect of resource efficiency, supporting continuous use without depletion of resources.

(ii) Compared to conventional water treatment methods, the use of NCs for adsorption offers a lower environmental footprint. NCs are inherently non-chemical substances and present a low risk of environmental contamination, thus ensuring minimal disturbance to aquatic ecosystems.

(iii) NCs exhibit high surface area and porosity, providing ample active sites for the adsorption of aquatic pollutants such as heavy metals, dyes, pesticides, and pharmaceuticals. Their efficient adsorption properties enable the effective removal of contaminants from water, contributing to improved water quality and ecosystem health.

(iv) NCs can often be regenerated and reused multiple times, further enhancing their sustainability in water treatment applications. Techniques such as thermal treatment, chemical regeneration, and rinsing allow for the recovery of adsorbed pollutants and the restoration of NC functionality, prolonging their lifespan and reducing waste generation.

(v) Due to its high compatibility, NCs can be integrated with other green technologies and sustainable practices in water treatment. For instance, NCs can be incorporated into bio-based materials for wastewater treatment processes, aligning with broader sustainability objectives.

(vi) The modification and treatment processes of NCs typically require minimal energy input compared to traditional adsorbents. Unlike energy-intensive methods such as chemical synthesis or membrane filtration, preparing NCs involves relatively simple procedures, such as intercalation, functionalization, or surface modification, which often occur under ambient conditions or moderate temperatures. These processes require minimal energy consumption, contributing to overall energy efficiency in water treatment applications. Additionally, using NCs as adsorbents eliminates the need for energy-intensive regeneration steps, as they can often be regenerated using simple techniques such as washing or heating, further reducing energy requirements. Therefore, NCs offer a sustainable solution for water treatment by saving energy throughout their lifecycle, from production to application and regeneration.

10. Challenges, recommendations, limitations, and future outlook

- A significant challenge in the application of NCs for water treatment is the lack of comprehensive sustainability assessments and life cycle analyses (LCA). The existing literature is sparse, and there is a pressing need for studies that evaluate the environmental impact, resource consumption, and long-term viability of NCs use across its entire lifecycle. This gap in the literature limits our understanding of the true sustainability of NCs, potentially hindering their adoption in large-scale water treatment applications. Hence, it is essential to conduct detailed sustainability assessments and life cycle analyses to evaluate the environmental and economic implications of NCs. These assessments should consider the entire lifecycle of NCs, from raw material extraction and synthesis to application, regeneration, and disposal.
- Research should prioritize evaluating the application and performance of NCs at an industrial scale, particularly in continuous adsorption systems like pilot fixed beds. While current studies predominantly focus on discontinuous systems, there is a critical need for further investigation into scalable applications to better understand and optimize the use of NCs in large-scale water treatment processes.
- The synthesis and modification of NCs require careful consideration, as while functionalization can improve adsorption properties, the use of certain chemicals may pose new environmental risks. Thus, it is essential to develop low-cost, eco-friendly methods for synthesizing and modifying NCs, ensuring that the benefits of enhanced adsorption do not come at the expense of environmental safety.
- The agglomeration of NC particles presents a significant challenge by reducing the available surface area for adsorption and impeding their dispersion in water, thereby limiting effectiveness. Therefore, research should focus on developing stable dispersions to maintain NCs' high surface area and reactivity, ensuring consistent performance in water treatment applications.
- Conducting economic analyses of the synthesis and modification of NCs is crucial, as only a few studies have addressed this aspect. Understanding the cost implications of these processes will provide valuable insights into the feasibility of scaling up NC applications for industrial water treatment.
- Integrating NCs with other treatment methods promises to enhance water pollution control performance. Further exploration into the combined use of NCs with various treatment methods could lead to more effective pollution control strategies, especially in large-scale applications.

11. Conclusion and remarks

The review provided a comprehensive overview of the utilization of NCs in water treatment, particularly focusing on the adsorption of aquatic pollutants. NCs offer significant promise as adsorbents due to their unique properties, including high surface area, tunable surface chemistry, and environmental compatibility. The discussion has highlighted various aspects of NC-based adsorption processes, including adsorption mechanisms, factors influencing adsorption efficiency, regeneration, and the sustainability of NC applications. Furthermore, the characterization of NCs was thoroughly examined and discussed, covering various analytical techniques and methodologies. Moreover, the potential for NCs to simultaneously adsorb diverse pollutants was also reviewed, underscoring their efficacy and capacity for holistic remediation of contaminated water. Challenges such as lack of comprehensive sustainability assessments, the need for in-depth analysis of adsorption phenomena, and the lack of full-scale application have been identified. However, future prospects remain promising, with opportunities for further research in areas such as NC modification, comparative economic analysis, and industrial-scale application. Therefore, NCs represent a valuable sorbent for efficient and sustainable water treatment solutions, with the potential to address pressing environmental challenges and contribute to the advancement of water treatment technologies. Hence, this review is expected to lay a solid foundation for future studies and improvements in NCs-based water remediation.

CRediT authorship contribution statement

Luiz Daniel da Silva Neto: Writing – original draft, Conceptualization. **Ali Maged:** Writing – review & editing, Writing – original draft, Conceptualization. **Rafaela Gabriel:** Writing – original draft. **Pollyanna V.S. Lins:** Writing – original draft. **Nils H. Haneklaus:** Writing – review & editing. **Mark W. Hlawitschka:** Writing – review & editing, Supervision. **Lucas Meili:** Writing – review & editing, Writing – original draft, Supervision.

Declaration of competing interest

The authors declare that they have no known competing financial interests or personal relationships that could have appeared to influence the work reported in this paper.

Data availability

Data will be made available on request.

Acknowledgments

The authors (A.M., N.H.H., and M.W.H.) are thankful for the support provided by Africa-UniNet, financed by the Austrian Federal Ministry of Education, Science and Research (BMBWF) and implemented by OeAD [Africa UNINET P056 and P119]. All authors sincerely express their appreciation and thanks to the editor and reviewers whose critical commentary has significantly improved the quality of this publication.

Appendix A. Supplementary data

Supplementary data to this article can be found online at https://doi.org/10.1016/j.jwpe.2024.106180.

References

[1] R. Kumar, M. Kumar, G. Luthra, Fundamental approaches and applications of nanotechnology: a mini review, Mater. Today Proc. (2023), https://doi.org/10.1016/j.matpr.2022.12.172.
[2] G. Cavallaro, G. Lazzara, E. Rozhina, S. Konnova, M. Kryuchkova, N. Khaertdinov, R. Fakhrullin, Organic-nanoclay composite materials as removal agents for environmental decontamination, RSC Adv. 9 (2019) 40553–40564, https://doi.org/10.1039/c9ra08230a.
[3] R. Iravani, C. An, Y. Adamian, M. Mohammadi, A review on the use of nanoclay adsorbents in environmental pollution control, Water Air Soil Pollut. 233 (2022) 1–17, https://doi.org/10.1007/s11270-022-05580-2.
[4] E. Pavón, R. Martín-Rodríguez, A.C. Perdigón, M.D. Alba, New trends in nanoclay-modified sensors, Inorganics 9 (2021) 43, https://doi.org/10.3390/inorganics9060043.
[5] D. López-Rodríguez, B. Micó-Vicent, J. Jordán-Núñez, M. Bonet-Aracil, E. Bou-Belda, Uses of nanoclays and adsorbents for dye recovery: a textile industry review, Appl. Sci. 11 (2021) 11422, https://doi.org/10.3390/app112311422.
[6] V. Vinayagam, S. Murugan, R. Kumaresan, M. Narayanan, M. Sillanpää, D. Viet N. Vo, O.S. Kushwaha, P. Jenis, P. Potdar, S. Gadiya, Sustainable adsorbents for the removal of pharmaceuticals from wastewater: a review, Chemosphere 300 (2022) 134597, https://doi.org/10.1016/j.chemosphere.2022.134597.
[7] D. Peixoto, I. Pereira, M. Pereira-Silva, F. Veiga, M.R. Hamblin, Y. Lvov, M. Liu, A.C. Paiva-Santos, Emerging role of nanoclays in cancer research, diagnosis, and therapy, Coord. Chem. Rev. 440 (2021) 213956, https://doi.org/10.1016/j.ccr.2021.213956.
[8] M.N. Uddin, M.T. Hossain, N. Mahmud, S. Aalm, M. Joaber, S.I. Mahedi, A. Ali, Research and applications of nanoclays: a review, SPE Polym. (2024), https://doi.org/10.1002/pls2.10146.
[9] X. Li, J. Ichiro Hayashi, C.Z. Li, FT-Raman spectroscopic study of the evolution of char structure during the pyrolysis of a Victorian brown coal, Fuel 85 (2006) 1700–1707, https://doi.org/10.1016/j.fuel.2006.03.008.

[10] K.S. Katti, H. Jasuja, S.V. Jaswandkar, S. Mohanty, D.R. Katti, Nanoclays in medicine: a new frontier of an ancient medical practice, Mater. Adv. 3 (2022) 7484–7500, https://doi.org/10.1039/d2ma00528j.
[11] F. Uddin, Clays, nanoclays, and montmorillonite minerals, Metall. Mater. Trans. A 39 (2008) 2804–2814, https://doi.org/10.1007/S11661-008-9603-5.
[12] S. Murugesan, T. Scheibel, Copolymer/clay nanocomposites for biomedical applications, Adv. Funct. Mater. 30 (2020) 201908101, https://doi.org/10.1002/adfm.201908101.
[13] D.O. Govea-Alonso, M.J. García-Soto, L. Betancourt-Mendiola, E. Padilla-Ortega, S. Rosales-Mendoza, O. González-Ortega, Nanoclays: promising materials for vaccinology, Vaccines 10 (2022) 1549, https://doi.org/10.3390/vaccines10091549.
[14] C.V. Lazaratou, D. Panagiotaras, G. Panagopoulos, M. Pospíšil, D. Papoulis, Ca treated palygorskite and halloysite clay minerals for ferrous iron (Fe+2) removal from water systems, Environ. Technol. Innov. 19 (2020) 100961, https://doi.org/10.1016/j.eti.2020.100961.
[15] C.E. Brunchi, S. Morariu, Laponite®—from dispersion to gel—structure, properties, and applications, Molecules 29 (2024) 105161, https://doi.org/10.3390/molecules29122823.
[16] R. Gahlot, K. Taki, M. Kumar, Efficacy of nanoclays as the potential adsorbent for dyes and metal removal from the wastewater: a review, Environ. Nanotechnol. Monit. Manag. 14 (2020) 100339, https://doi.org/10.1016/j.enmm.2020.100339.
[17] R. Rafiee, R. Shahzadi, Mechanical properties of nanoclay and nanoclay reinforced polymers: a review, Polym. Compos. 40 (2019) 431–445, https://doi.org/10.1002/pc.24725.
[18] A. Maged, S. Kharbish, I.S.I.S. Ismael, A. Bhatnagar, Characterization of activated bentonite clay mineral and the mechanisms underlying its sorption for ciprofloxacin from aqueous solution, Environ. Sci. Pollut. Res. 27 (2020) 32980–32997, https://doi.org/10.1007/s11356-020-09267-1.
[19] É. Teixeira-Neto, A.A. Teixeira-Neto, Chemical modification of clays: scientific and technological chalenges for obtaining new value added products, Quim Nova 32 (2009) 809–817, https://doi.org/10.1590/s0100-40422009000300023.
[20] L. Fu, H. Yang, A. Tang, Y. Hu, Engineering a tubular mesoporous silica nanocontainer with well-preserved clay shell from natural halloysite, Nano Res. 10 (2017) 2782–2799, https://doi.org/10.1007/s12274-017-1482-x.
[21] S.M. Lee, D. Tiwari, Organo and inorgano-organo-modified clays in the remediation of aqueous solutions: an overview, Appl. Clay Sci. 59–60 (2012) 84–102, https://doi.org/10.1016/j.clay.2012.02.006.
[22] A.F. Baruel, R.C.L. Dutra, M.R. Baldan, C.M.A. Lopes, S.N. Cassu, Organophilization and silanization of bentonite clay, Quim Nova 41 (2018) 134–139, https://doi.org/10.21577/0100-4042.20170160.
[23] M.M. Takematsu, A.F. Baruel, S.N. Cassu, M.F. Diniz, D.A. Graves, R. de Cássia Lazzarini Dutra, Development and characterization of sodium polyacrylate/bentonite hydrogel with epoxy resin coating, Polimeros 33 (2023) e20230021, https://doi.org/10.1590/0104-1428.20230029.
[24] A.F. Baruel, R.C.L. Dutra, M.F. Diniz, M.F.P. Azevedo, S.N. Cassu, The role of organoclay in the diffusion of epoxy-amine oligomers and in the cross-linking density of the resulting network, J. Appl. Polym. Sci. 140 (2023) e53571, https://doi.org/10.1002/app.53571.
[25] S. Adrar, A. Habi, A. Ajji, Y. Grohens, Synergistic effects in epoxy functionalized graphene and modified organo-montmorillonite PLA/PBAT blends, Appl. Clay Sci. 157 (2018) 65–75, https://doi.org/10.1016/j.clay.2018.02.028.
[26] L.B. de Paiva, A.R. Morales, F.R. Valenzuela Díaz, Organoclays: properties, preparation and applications, Appl. Clay Sci. 42 (2008) 8–24, https://doi.org/10.1016/J.CLAY.2008.02.006.
[27] I.K. Breakwell, J. Homer, M.A.M. Lawrence, W.R. McWhinnie, Studies of organophilic clays: the distribution of quaternary ammonium compounds on clay surfaces and the role of impurities, Polyhedron 14 (1995) 2511–2518, https://doi.org/10.1016/0277-5387(95)00053-U.
[28] S. Yoshimoto, F. Ohashi, T. Kameyama, X-ray diffraction studies of intercalation compounds prepared from aniline salts and montmorillonite by a mechanochemical processing, Solid State Commun. 136 (2005) 251–256, https://doi.org/10.1016/j.ssc.2005.08.017.
[29] D. Merinska, Z. Malac, M. Pospisil, Z. Weiss, M. Chmielova, P. Capkova, J. Simonik, Polymer/clay nanocomposites based on MMT/ODA intercalates, Compos. Interfaces 9 (2002) 529–540, https://doi.org/10.1163/15685540260494100.
[30] H. He, Q. Tao, J. Zhu, P. Yuan, W. Shen, S. Yang, Silylation of clay mineral surfaces, Appl. Clay Sci. 71 (2013) 15–20, https://doi.org/10.1016/j.clay.2012.09.028.
[31] L.N.F. Queiroga, M.B.B. Pereira, L.S. Silva, E.C. Silva Filho, I.M.G. Santos, M. G. Fonseca, T. Georgelin, M. Jaber, Microwave bentonite silylation for dye removal: influence of the solvent, Appl. Clay Sci. 168 (2019) 478–487, https://doi.org/10.1016/j.clay.2018.11.027.
[32] H. Abbassi, R. Abidi, M. Benna-Zayani, Synthesis, characterization and chromium ions adsorption of the nanocomposite calix[6]arene-tetraester-silylated-clay, Chem. Phys. Lett. 833 (2023) 140918, https://doi.org/10.1016/j.cplett.2023.140918.
[33] P.T. Bertuoli, D. Piazza, L.C. Scienza, A.J. Zattera, Preparation and characterization of montmorillonite modified with 3-aminopropyltriethoxysilane, Appl. Clay Sci. 87 (2014) 46–51, https://doi.org/10.1016/j.clay.2013.11.020.
[34] A. Di Gianni, E. Amerio, O. Monticelli, R. Bongiovanni, Preparation of polymer/clay mineral nanocomposites via dispersion of silylated montmorillonite in a UV curable epoxy matrix, Appl. Clay Sci. 42 (2008) 116–124, https://doi.org/10.1016/j.clay.2007.12.011.
[35] K. Isoda, K. Kuroda, M. Ogawa, Interlamellar grafting of γ-methacryloxypropylsilyl groups on magadiite and copolymerization with methyl methacrylate, Chem. Mater. 12 (2000) 1702–1707, https://doi.org/10.1021/cm0000494.
[36] M.A. Vicente, A. Gil, F. Bergaya, Pillared Clays and Clay Minerals, in: Dev. Clay Sci, Elsevier, 2013, pp. 523–557, https://doi.org/10.1016/B978-0-08-098258-8.00017-1.
[37] R.A. Schoonheydt, T. Pinnavaia, G. Lagaly, N. Gangas, Pillared clays and pillared layered solids (technical report), Pure Appl. Chem. 71 (1999) 2367–2371, https://doi.org/10.1351/pac199971122367.
[38] G.D. Corte, F.F. Pinto, M.T. Stefanello, C. Gulart, J.P. de Ramos, R.S. Balardin, Technology application technology of pesticides for control of soybean nematodes, Cienc. Rural 44 (2014) 1534–1540, https://doi.org/10.1590/0103-8478cr20131536.
[39] H. Desai, K. A, G.S.K. Reddy, Sustainable and rapid pillared clay synthesis with applications in removal of anionic and cationic dyes, Microporous Mesoporous Mater. 352 (2023) 112488, https://doi.org/10.1016/j.micromeso.2023.112488.
[40] P. Liu, Polymer modified clay minerals: a review, Appl. Clay Sci. 38 (2007) 64–76, https://doi.org/10.1016/j.clay.2007.01.004.
[41] P. Moradihamedani, Recent development in polymer/montmorillonite clay mixed matrix membranes for gas separation: a short review, Polym. Bull. 80 (2023) 4663–4687, https://doi.org/10.1007/s00289-022-04266-3.
[42] F. Guo, S. Aryana, Y. Han, Y. Jiao, A review of the synthesis and applications of polymer–nanoclay composites, Appl. Sci. 8 (2018) 1696, https://doi.org/10.3390/app8091696.
[43] K. Buruga, J.T. Kalathi, A facile synthesis of halloysite nanotubes based polymer nanocomposites for glass coating application, J. Alloys Compd. 735 (2018) 1807–1817, https://doi.org/10.1016/j.jallcom.2017.11.211.
[44] G. Coativy, M. Misra, A.K. Mohanty, Microwave synthesis and melt blending of glycerol based toughening agent with poly(lactic acid), ACS Sustain. Chem. Eng. 4 (2016) 2142–2149, https://doi.org/10.1021/acssuschemeng.5b01596.
[45] M. Hesami, A. Jalali-Arani, Morphology development via static crosslinking of (polylactic acid/acrylic rubber) as an immiscible polymer blend, Macromol. Mater. Eng. 303 (2018) 1700446, https://doi.org/10.1002/mame.201700446.
[46] R.I. Narro-Céspedes, M.G. Neira-Velázquez, L.F. Mora-Cortes, E. Hernández-Hernández, A.O. Castañeda-Facio, M.C. Ibarra-Alonso, Y.K. Reyes-Acosta, G. Soria-Arguello, J.J. Borjas-Ramos, Surface modification of sodium montmorillonite nanoclay by plasma polymerization and its effect on the properties of polystyrene nanocomposites, J. Nanomater. 2018 (2018) 2480798, https://doi.org/10.1155/2018/2480798.
[47] S. Sinha Ray, Rheology of polymer/layered silicate nanocomposites, J. Ind. Eng. Chem. 12 (2006) 811–842.
[48] E.T. Thostenson, C. Li, T.W. Chou, Nanocomposites in context, Compos. Sci. Technol. 65 (2005) 491–516, https://doi.org/10.1016/j.compscitech.2004.11.003.
[49] H. Baniasadi, S.A. A. Ramazani, S. Javan Nikkhah, A. Ramazani, S. Javan Nikkhah, Investigation of in situ prepared polypropylene/clay nanocomposites properties and comparing to melt blending method, Mater. Des. 31 (2010) 76–84, https://doi.org/10.1016/j.matdes.2009.07.014.
[50] U. Kuila, M. Prasad, Specific surface area and pore-size distribution in clays and shales, Geophys. Prospect. 61 (2013) 341–362, https://doi.org/10.1111/1365-2478.12028.
[51] M.J. Avena, C.P. De Pauli, Proton adsorption and electrokinetics of an Argentinean montmorillonite, J. Colloid Interface Sci. 202 (1998) 195–204, https://doi.org/10.1006/jcis.1998.5402.
[52] L. Ammann, F. Bergaya, G. Lagaly, Determination of the cation exchange capacity of clays with copper complexes revisited, Clay Miner. 40 (2005) 441–453, https://doi.org/10.1180/0009855054040182.
[53] S. Sen Gupta, K.G. Bhattacharyya, Adsorption of heavy metals on kaolinite and montmorillonite: a review, Phys. Chem. Chem. Phys. 14 (2012) 6698–6723, https://doi.org/10.1039/c2cp40093f.
[54] M. Kosmulski, The pH dependent surface charging and points of zero charge. VII. Update, Adv. Colloid Interf. Sci. 251 (2018) 115–138, https://doi.org/10.1016/j.cis.2017.10.005.
[55] M. Kryuchkova, S. Batasheva, F. Akhatova, V. Babaev, D. Buzyurova, A. Vikulina, D. Volodkin, R. Fakhrullin, E. Rozhina, Pharmaceuticals removal by adsorption with montmorillonite nanoclay, Int. J. Mol. Sci. 22 (2021) 9670, https://doi.org/10.3390/ijms22189670.
[56] Y. Zhang, M. Long, P. Huang, H. Yang, S. Chang, Y. Hu, A. Tang, L. Mao, Emerging integrated nanoclay-facilitated drug delivery system for papillary thyroid cancer therapy, Sci. Rep. 6 (2016) 1–10, https://doi.org/10.1038/srep33335.
[57] B.T. Ribeiro, J.M. De Lima, N. Curi, G.C. De Oliveira, P.L.T. Lima, Surface charge of clay fraction as affected by vinasse and phosphorus, Quim Nova 34 (2011) 5–10, https://doi.org/10.1590/s0100-40422011000100002.
[58] X. Zhang, X. Wang, Adsorption and desorption of Nickel(II) ions from aqueous solution by a lignocellulose/montmorillonite nanocomposite, PLoS One 10 (2015) 1–21, https://doi.org/10.1371/journal.pone.0117077.
[59] S. Ramanayaka, B. Sarkar, A.T. Cooray, Y.S. Ok, M. Vithanage, Halloysite nanoclay supported adsorptive removal of oxytetracycline antibiotic from aqueous media, J. Hazard. Mater. 384 (2020) 121301, https://doi.org/10.1016/j.jhazmat.2019.121301.
[60] P. Das, S. Manna, A.K. Behera, M. Shee, P. Basak, A.K. Sharma, Current synthesis and characterization techniques for clay-based polymer nano-composites and its biomedical applications: a review, Environ. Res. 212 (2022) 113534, https://doi.org/10.1016/j.envres.2022.113534.

[61] N. Karak, Fundamentals of Nanomaterials and Polymer Nanocomposites, in: Nanomater. Polym. Nanocomposites Raw Mater. to Appl, Elsevier Inc., 2019, pp. 1–45, https://doi.org/10.1016/B978-0-12-814615-6.00001-1.
[62] J. Qu, Research progress of novel adsorption processes in water purification: a review, J. Environ. Sci. 20 (2008) 1–13, https://doi.org/10.1016/S1001-0742(08)60001-7.
[63] A. Maged, H.A. El-Fattah, R.M. Kamel, S. Kharbish, A.M. Elgarahy, A comprehensive review on sustainable clay-based geopolymers for wastewater treatment: circular economy and future outlook, Environ. Monit. Assess. 195 (2023) 693, https://doi.org/10.1007/s10661-023-11303-9.
[64] R. Yousef, H. Qiblawey, M.H. El-Naas, Adsorption as a process for produced water treatment: a review, Processes 8 (2020) 1–22, https://doi.org/10.3390/pr8121657.
[65] T. Zhang, W. Wang, Y. Zhao, H. Bai, T. Wen, S. Kang, G. Song, S. Song, S. Komarneni, Removal of heavy metals and dyes by clay-based adsorbents: from natural clays to 1D and 2D nano-composites, Chem. Eng. J. 420 (2021) 127574, https://doi.org/10.1016/j.cej.2020.127574.
[66] B. Prasad Ahirvar, P. Das, V. Srivastava, M. Kumar, Perspectives of heavy metal pollution indices for soil, sediment, and water pollution evaluation: an insight, Total Environ. Res. Themes 6 (2023) 100039, https://doi.org/10.1016/j.totert.2023.100039.
[67] N.S. Aljohani, Y.N. Kavil, R.K. Al-Farawati, S. Saad Alelyani, M.I. Orif, Y. A. Shaban, S.R. Al-Mhyawi, E.H. Aljuhani, M. Abdel Salam, The effective adsorption of arsenic from polluted water using modified Halloysite nanoclay, Arab. J. Chem. 16 (2023) 104652, https://doi.org/10.1016/j.arabjc.2023.104652.
[68] F. Hamidi, A.N. Baghani, M. Kasraee, M. Salari, M.H. Mehdinejad, Modeling, optimization and efficient use of MMT K10 nanoclay for Pb (II) removal using RSM, ANN and GA, Sci. Rep. 13 (2023) 1–13, https://doi.org/10.1038/s41598-023-35709-0.
[69] M.E.-S. Abdel-Raouf, R.S. Kamal, D.E. Hegazy, A. Sayed, Gamma irradiation synthesis of carboxymethyl chitosan-nanoclay hydrogel for the removal of Cr(VI) and Pb(II) from aqueous media, J. Inorg. Organomet. Polym. Mater. 33 (2023) 895–913, https://doi.org/10.1007/s10904-023-02543-w.
[70] Z. Wang, H. Tian, J. Liu, J. Wang, Q. Lu, L. Xie, Facet-dependent adsorption of heavy metal ions on Janus clay nanosheets, J. Hazard. Mater. 461 (2024) 132548, https://doi.org/10.1016/j.jhazmat.2023.132548.
[71] H. Rasoulzadeh, M.H. Dehghani, A.S. Mohammadi, R.R. Karri, R. Nabizadeh, S. Nazmara, K.H. Kim, J.N. Sahu, Parametric modelling of Pb(II) adsorption onto chitosan-coated Fe3O4 particles through RSM and DE hybrid evolutionary optimization framework, J. Mol. Liq. 297 (2020) 111893, https://doi.org/10.1016/j.molliq.2019.111893.
[72] H. Wang, S. Wang, S. Wang, L. Fu, L. Zhang, The one-step synthesis of a novel metal–organic frameworks for efficient and selective removal of Cr(VI) and Pb(II) from wastewater: kinetics, thermodynamics and adsorption mechanisms, J. Colloid Interface Sci. 640 (2023) 230–245, https://doi.org/10.1016/j.jcis.2023.02.108.
[73] D. Choque-Quispe, C.A. Ligarda-Samanez, B.S. Ramos-Pacheco, A.M. Solano-Reynoso, J. Quispe-Marcatoma, Y. Choque-Quispe, D.E. Peralta-Guevara, E. L. Martínez-Huamán, O. Correa-Cuba, M.L. Masco-Arriola, W.J. Lechuga-Canal, F. Montalvo Amanca, Formulation of novel composite (activated nanoclay/hydrocolloid of nostoc sphaericum) and its application in the removal of heavy metals from wastewater, Polymers (Basel) 14 (2022) 2803, https://doi.org/10.3390/polym14142803.
[74] Z.H. Huang, X. Zheng, W. Lv, M. Wang, Q.H. Yang, F. Kang, Adsorption of lead(II) ions from aqueous solution on low-temperature exfoliated graphene nanosheets, Langmuir 27 (2011) 7558–7562, https://doi.org/10.1021/la200606r.
[75] L.P. Lingamdinne, O. Amelirad, J.R. Koduru, R.R. Karri, Y.Y. Chang, M. H. Dehghani, N.M. Mubarak, Functionalized bentonite for removal of Pb(II) and As(V) from surface water: predicting capability and mechanism using artificial neural network, J. Water Process Eng. 51 (2023) 103386, https://doi.org/10.1016/j.jwpe.2022.103386.
[76] F.I.A.M. Aisha Muthana Alasadi, Adsorption of Cu(II), Ni(II) and Zn(II) ions by nano kaolinite: thermodynamics and kinetics studies, Chem. Int.)-. 5((2019) 258–268, https://doi.org/10.5281/zenodo.2644985.
[77] F. Batool, A. Mohyuddin, A. Amjad, A. ul Hassan, S. Nadeem, M. Javed, M. Hafiz Dzarfan Othman, K. Wayne Chew, A. Rauf, T.A. Kurniawan, Removal of Cd(II) and Pb(II) from synthetic wastewater using Rosa damascena waste as a biosorbent: an insight into adsorption mechanisms, kinetics, and thermodynamic studies, Chem. Eng. Sci. 280 (2023) 119072, https://doi.org/10.1016/j.ces.2023.119072.
[78] M. Geszke-Moritz, M. Moritz, APTES-modified mesoporous silicas as the carriers for poorly water-soluble drug. Modeling of diflunisal adsorption and release, Appl. Surf. Sci. 368 (2016) 348–359, https://doi.org/10.1016/j.apsusc.2016.02.004.
[79] R. Pelalak, Z. Heidari, S.M. Khatami, T.A. Kurniawan, A. Marjani, S. Shirazian, Oak wood ash/GO/Fe3O4 adsorption efficiencies for cadmium and lead removal from aqueous solution: kinetics, equilibrium and thermodynamic evaluation, Arab. J. Chem. 14 (2021) 102991, https://doi.org/10.1016/j.arabjc.2021.102991.
[80] S. Rajput, C.U. Pittman, D. Mohan, Magnetic magnetite (Fe3O4) nanoparticle synthesis and applications for lead (Pb2+) and chromium (Cr6+) removal from water, J. Colloid Interface Sci. 468 (2016) 334–346, https://doi.org/10.1016/j.jcis.2015.12.008.
[81] Ş. Yılmaz, A. Zengin, T. Şahan, Ö.S. Zorer, Utilization of a novel polymer–clay material for high elimination of hazardous radioactive contamination uranium (VI) from aqueous environments, Environ. Technol. Innov. 23 (2021) 101631, https://doi.org/10.1016/j.eti.2021.101631.
[82] R. Novikau, G. Lujaniene, Adsorption behaviour of pollutants: heavy metals, radionuclides, organic pollutants, on clays and their minerals (raw, modified and treated): a review, J. Environ. Manag. 309 (2022) 114685, https://doi.org/10.1016/j.jenvman.2022.114685.
[83] Y.H. Cai, X.J. Yang, A.I. Schäfer, Removal of naturally occurring strontium by nanofiltration/reverse osmosis from groundwater, Membranes (Basel) 10 (2020) 1–23, https://doi.org/10.3390/membranes10110321.
[84] T. Missana, M. Garcia-Gutierrez, U. Alonso, Sorption of strontium onto illite/smectite mixed clays, Phys. Chem. Earth 33 (2008) S156–S162, https://doi.org/10.1016/j.pce.2008.10.020.
[85] A.-A.M. Abdel-Karim, A.A. Zaki, W. Elwan, M.R. El-Naggar, M.M. Gouda, Experimental and modeling investigations of cesium and strontium adsorption onto clay of radioactive waste disposal, Appl. Clay Sci. 132–133 (2016) 391–401, https://doi.org/10.1016/j.clay.2016.07.005.
[86] T. Thiebault, J. Brendlé, G. Augé, L. Limousy, Cleaner synthesis of silylated clay minerals for the durable recovery of ions (Co2+ and Sr2+) from aqueous solutions, Ind. Eng. Chem. Res. 59 (2020) 2104–2112, https://doi.org/10.1021/acs.iecr.9b06118.
[87] Y. Izosimova, I. Gurova, I. Tolpeshta, M. Karpukhin, S. Zakusin, O. Zakusina, A. Samburskiy, V. Krupskaya, Adsorption of Cs(I) and Sr(II) on bentonites with different compositions at different pH, Minerals 12 (2022) 862, https://doi.org/10.3390/min12070862.
[88] H. Wu, S. Lin, X. Cheng, J. Chen, Y. Ji, D. Xu, M. Kang, Comparative study of strontium adsorption on muscovite, biotite and phlogopite, J. Environ. Radioact. 225 (2020) 106446, https://doi.org/10.1016/j.jenvrad.2020.106446.
[89] V. Tobilko, L. Spasonova, I. Kovalchuk, B. Kornilovych, Y. Kholodko, Adsorption of uranium (Vi) from aqueous solutions by amino-functionalized clay minerals, Colloids Interfaces 3 (2019) 41, https://doi.org/10.3390/colloids3010041.
[90] G. Bernhard, G. Geipel, T. Reich, V. Brendler, S. Amayri, H. Nitsche, H. Nitsche, Uranyl(VI) carbonate complex formation: validation of the Ca2UO2(CO3)3(aq.) species, Radiochim. Acta 89 (2001) 511, https://doi.org/10.1524/ract.2001.89.8.511.
[91] F. Li, Z. Gao, X. Li, L. Fang, The effect of Paecilomyces catenlannulatus on removal of U(VI) by illite, J. Environ. Radioact. 137 (2014) 31–36, https://doi.org/10.1016/j.jenvrad.2014.06.014.
[92] T.S. Anirudhan, J.R. Deepa, Binusreejayan, Synthesis and characterization of multi-carboxyl-functionalized nanocellulose/nanobentonite composite for the adsorption of uranium(VI) from aqueous solutions: kinetic and equilibrium profiles, Chem. Eng. J. 273 (2015) 390–400, https://doi.org/10.1016/j.cej.2015.03.007.
[93] E. Ordoñez-Regil, H.B. Ortíz-Oliveros, S.M. Fernández-Valverde, F. Granados-Correa, Eu (III) sorption from an aqueous solution onto SrTiO3 and surface complex behavior, Chem. Eng. J. 254 (2014) 349–356, https://doi.org/10.1016/j.cej.2014.05.130.
[94] T. Missana, U. Alonso, M. García-Gutiérrez, Evaluation of component additive modelling approach for europium adsorption on 2:1 clays: experimental, thermodynamic databases, and models, Chemosphere 272 (2021) 129877, https://doi.org/10.1016/j.chemosphere.2021.129877.
[95] G. Lujanienė, R. Novikau, K. Karalevičiūtė, V. Pakštas, M. Talaikis, L. Levinskaitė, A. Selskienė, A. Selskis, J. Mažeika, K. Jokšas, Chitosan-minerals-based composites for adsorption of caesium, cobalt and europium, J. Hazard. Mater. 462 (2024) 132747, https://doi.org/10.1016/j.jhazmat.2023.132747.
[96] H. Ma, F. Zhang, Q. Li, G. Chen, S. Hu, H. Cheng, Preparation of ZnO nanoparticle loaded amidoximated wool fibers as a promising antibiofouling adsorbent for uranium(vi) recovery, RSC Adv. 9 (2019) 18406–18414, https://doi.org/10.1039/c9ra03777b.
[97] A.A. Younes, A.M. Masoud, M.H. Taha, Uranium sorption from aqueous solutions using polyacrylamide-based chelating sorbents, Sep. Sci. Technol. 53 (2018) 2573–2586, https://doi.org/10.1080/01496395.2018.1467450.
[98] W.M. Youssef, A.E.M. Hussein, M.H. Taha, M.M. El-Maadawy, Uranium(VI) sorption from liquid waste solution using functionalized polyurethane polymer: kinetic and isotherm characterizations, Russ. J. Inorg. Chem. 67 (2022) 1058–1068, https://doi.org/10.1134/S0036023622070245.
[99] F.I. Khalili, N.H. Salameh, M.M. Shaybe, Sorption of uranium(VI) and thorium (IV) by Jordanian bentonite, J. Chem. 2013 (2013) 1–13, https://doi.org/10.1155/2013/586136.
[100] O.E. Roshdy, Removal of uranium, cadmium and iron ions from phosphoric acid solution using amberjet 1200 H resin: an experimental, isotherm and kinetic study, J. Radioanal. Nucl. Chem. 329 (2021) 85–101, https://doi.org/10.1007/s10967-021-07792-y.
[101] S. Dai, N. Wang, C. Qi, X. Wang, Y. Ma, L. Yang, X. Liu, Q. Huang, C. Nie, B. Hu, X. Wang, Preparation of core-shell structure Fe3O4@C@MnO2 nanoparticles for efficient elimination of U(VI) and Eu(III) ions, Sci. Total Environ. 685 (2019) 986–996, https://doi.org/10.1016/j.scitotenv.2019.06.292.
[102] E.S.A. Haggag, A.A. Abdelsamad, A.M. Masoud, Potentiality of uranium extraction from acidic leach liquor by polyacrylamide-acrylic acid titanium silicate composite adsorbent, Int. J. Environ. Anal. Chem. 100 (2020) 204–224, https://doi.org/10.1080/03067319.2019.1636037.
[103] X. Zhang, L. Ji, J. Wang, R. Li, Q. Liu, M. Zhang, L. Liu, Removal of uranium(VI) from aqueous solutions by magnetic Mg-Al layered double hydroxide intercalated with citrate: kinetic and thermodynamic investigation, Colloids Surf. A: Physicochem. Eng. Asp. 414 (2012) 220–227, https://doi.org/10.1016/j.colsurfa.2012.08.031.

[104] F. Liu, Y. Lou, F. Xia, B. Hu, Immobilizing nZVI particles on MBenes to enhance the removal of U(VI) and Cr(VI) by adsorption-reduction synergistic effect, Chem. Eng. J. 454 (2023) 140318, https://doi.org/10.1016/j.cej.2022.140318.
[105] A. Pandey, S. Govindwar, M. Kurade, B. Jeon, Current Developments in Bioengineering and Biotechnology: Advances in Eco-friendly and Sustainable Technologies for the Treatment of Textile Wastewater, Elsevier, 2023.
[106] M.A. Salam, S.A. Kosa, A.A. Al-Beladi, Application of nanoclay for the adsorptive removal of Orange G dye from aqueous solution, J. Mol. Liq. 241 (2017) 469–477, https://doi.org/10.1016/j.molliq.2017.06.055.
[107] A. Hassani, A. Khataee, S. Karaca, M. Karaca, M. Kıranşan, M. Kiranşan, Adsorption of two cationic textile dyes from water with modified nanoclay: a comparative study by using central composite design, J. Environ. Chem. Eng. 3 (2015) 2738–2749, https://doi.org/10.1016/j.jece.2015.09.014.
[108] L.A. Arni, A. Hapiz, A.H. Jawad, A.S. Abdulhameed, Z.A. ALOthman, L.D. Wilson, Fabrication of magnetic chitosan-grafted salicylaldehyde/nanoclay for removal of azo dye: BBD optimization, characterization, and mechanistic study, Int. J. Biol. Macromol. 248 (2023) 125943, https://doi.org/10.1016/j.ijbiomac.2023.125943.
[109] H.S. Far, M. Hasanzadeh, M. Najafi, R. Rahimi, Hybridization of nanoclay with a chromium-based metal-organic framework for boosting adsorption of organic dyes from wastewater, ChemistrySelect 7 (2022) e202104191, https://doi.org/10.1002/slct.202104191.
[110] G.B. Marandi, M. Baharloui, M. Kurdtabar, L.M. Sharabian, M.A. Mojarrad, Hydrogel with high laponite content as nanoclay: swelling and cationic dye adsorption properties, Res. Chem. Intermed. 41 (2015) 7043–7058, https://doi.org/10.1007/s11164-014-1797-0.
[111] J.N. Edokpayi, S.S. Ndlovu, J.O. Odiyo, Characterization of pulverized Marula seed husk and its potential for the sequestration of methylene blue from aqueous solution, BMC Chem. 13 (2019) 1–14, https://doi.org/10.1186/s13065-019-0530-x.
[112] Y. Jin, C. Zeng, Q.F. Lü, Y. Yu, Efficient adsorption of methylene blue and lead ions in aqueous solutions by 5-sulfosalicylic acid modified lignin, Int. J. Biol. Macromol. 123 (2019) 50–58, https://doi.org/10.1016/j.ijbiomac.2018.10.213.
[113] N. Peng, D. Hu, J. Zeng, Y. Li, L. Liang, C. Chang, Superabsorbent cellulose-clay nanocomposite hydrogels for highly efficient removal of dye in water, ACS Sustain. Chem. Eng. 4 (2016) 7217–7224, https://doi.org/10.1021/acssuschemeng.6b02178.
[114] K. Saini, A. Maged, A. Sahoo, T. Bhaskar, K.K. Pant, A. Bhatnagar, A novel lignin-steel sludge composite for dyes adsorption from water: surface functionalities and structural alteration mechanisms, J. Water Process Eng. 64 (2024) 105600, https://doi.org/10.1016/J.JWPE.2024.105600.
[115] H. Ma, J.B. Li, W.W. Liu, M. Miao, B.J. Cheng, S.W. Zhu, Novel synthesis of a versatile magnetic adsorbent derived from corncob for dye removal, Bioresour. Technol. 190 (2015) 13–20, https://doi.org/10.1016/j.biortech.2015.04.048.
[116] R. Zein, J.S. Purnomo, P. Ramadhani, M.F. Alif, S. Safni, Lemongrass (Cymbopogon nardus) leaves biowaste as an effective and low-cost adsorbent for methylene blue dyes removal: isotherms, kinetics, and thermodynamics studies, Sep. Sci. Technol. 57 (2022) 2341–2357, https://doi.org/10.1080/01496395.2022.2058549.
[117] M.A. Franciski, E.C. Peres, M. Godinho, D. Perondi, E.L. Foletto, G.C. Collazzo, G. L. Dotto, Development of CO2 activated biochar from solid wastes of a beer industry and its application for methylene blue adsorption, Waste Manag. 78 (2018) 630–638, https://doi.org/10.1016/j.wasman.2018.06.040.
[118] M.F.M. Yusop, M.A. Ahmad, N.A. Rosli, M.E.A. Manaf, Adsorption of cationic methylene blue dye using microwave-assisted activated carbon derived from acacia wood: optimization and batch studies, Arab. J. Chem. 14 (2021) 103122, https://doi.org/10.1016/j.arabjc.2021.103122.
[119] S. Madduri, I. Elsayed, E.B. Hassan, Novel oxone treated hydrochar for the removal of Pb(II) and methylene blue (MB) dye from aqueous solutions, Chemosphere 260 (2020) 127683, https://doi.org/10.1016/j.chemosphere.2020.127683.
[120] D.L. Zhao, W. Zhou, L. Shen, B. Li, H. Sun, Q. Zeng, C.Y. Tang, H. Lin, T.S. Chung, New directions on membranes for removal and degradation of emerging pollutants in aqueous systems, Water Res. 251 (2024) 121111, https://doi.org/10.1016/j.watres.2024.121111.
[121] H. Abd El-Fattah, A. Maged, R.M. Kamel, S. Kharbish, Recent technologies for the elimination of pharmaceutical compounds from aqueous solutions: a review, Front. Sci. Res. Technol. 5 (2023) 0, https://doi.org/10.21608/FSRT.2023.173676.1074.
[122] H. Khamooshi, B. Dahrazma, A. Ebrahimi, S. Davoodi, A batch study on the adsorption/desorption behavior of vancomycin on bentonite nanoparticles in aqueous solutions, Water Sci. Technol. 82 (2020) 2603–2612, https://doi.org/10.2166/wst.2020.499.
[123] A. Maged, A.M. Elgarahy, M.W. Hlawitschka, N.H. Haneklaus, A.K. Gupta, A. Bhatnagar, Synergistic mechanisms for the superior sorptive removal of aquatic pollutants via functionalized biochar-clay composite, Bioresour. Technol. 387 (2023) 129593, https://doi.org/10.1016/j.biortech.2023.129593.
[124] T.M.S. Attia, X.L. Hu, D.Q. Yin, Synthesized magnetic nanoparticles coated zeolite for the adsorption of pharmaceutical compounds from aqueous solution using batch and column studies, Chemosphere 93 (2013) 2076–2085, https://doi.org/10.1016/j.chemosphere.2013.07.046.
[125] T. Gupta, M. Ratandeep, B. Dutt, S. Kaur, S. Punia, Sharma, P.K. Sahu, Pooja, L. Saya, Graphene-based nanomaterials as potential candidates for environmental mitigation of pesticides, Talanta 272 (2024) 125748, https://doi.org/10.1016/J.TALANTA.2024.125748.
[126] V.M. Pathak, V.K. Verma, B.S. Rawat, B. Kaur, N. Babu, A. Sharma, S. Dewali, M. Yadav, R. Kumari, S. Singh, A. Mohapatra, V. Pandey, N. Rana, J.M. Cunill, Current status of pesticide effects on environment, human health and it's eco-friendly management as bioremediation: a comprehensive review, Front. Microbiol. 13 (2022) 962619, https://doi.org/10.3389/fmicb.2022.962619.
[127] F. Khezami, O. Gómez-Navarro, M.V. Barbieri, N. Khiari, A. Chkirbene, S. Chiron, S. Khadhar, S. Pérez, Occurrence of contaminants of emerging concern and pesticides and relative risk assessment in Tunisian groundwater, Sci. Total Environ. 906 (2024) 167319, https://doi.org/10.1016/j.scitotenv.2023.167319.
[128] T.P.A. Shabeer, A. Saha, V.T. Gajbhiye, S. Gupta, K.M. Manjaiah, E. Varghese, Exploitation of nano-bentonite, nano-halloysite and organically modified nano-montmorillonite as an adsorbent and coagulation aid for the removal of multi-pesticides from water: a sorption modelling approach, Water Air Soil Pollut. 226 (2015) 1–14, https://doi.org/10.1007/s11270-015-2331-8.
[129] M. Shirzad-Siboni, A. Khataee, A. Hassani, S. Karaca, Preparation, characterization and application of a CTAB-modified nanoclay for the adsorption of an herbicide from aqueous solutions: kinetic and equilibrium studies, Comptes Rendus. Chim. 18 (2015) 204–214, https://doi.org/10.1016/j.crci.2014.06.004.
[130] D.A. Palacio, B.F. Urbano, B.L. Rivas, Application of nanocomposite polyelectrolytes for the removal of antibiotics as emerging pollutants in water, J. Water Process Eng. 46 (2022) 102582, https://doi.org/10.1016/j.jwpe.2022.102582.
[131] P. Tabrizian, W. Ma, A. Bakr, M.S. Rahaman, pH-sensitive and magnetically separable Fe/Cu bimetallic nanoparticles supported by graphene oxide (GO) for high-efficiency removal of tetracyclines, J. Colloid Interface Sci. 534 (2019) 549–562, https://doi.org/10.1016/j.jcis.2018.09.034.
[132] T. Ahamad, M. Naushad, T. Al-Shahrani, N. Al-hokbany, S.M. Alshehri, Preparation of chitosan based magnetic nanocomposite for tetracycline adsorption: kinetic and thermodynamic studies, Int. J. Biol. Macromol. 147 (2020) 258–267, https://doi.org/10.1016/j.ijbiomac.2020.01.025.
[133] G.A. Haghighat, M.H. Saghi, I. Anastopoulos, A. Javid, A. Roudbari, S.S. Talebi, S. K. Ghadiri, D.A. Giannakoudakis, M. Shams, Aminated graphitic carbon derived from corn stover biomass as adsorbent against antibiotic tetracycline: optimizing the physicochemical parameters, J. Mol. Liq. 313 (2020) 113523, https://doi.org/10.1016/j.molliq.2020.113523.
[134] A.O. Ifebajo, A.A. Oladipo, M. Gazi, Efficient removal of tetracycline by CoO/CuFe 2 O 4 derived from layered double hydroxides, Environ. Chem. Lett. 17 (2019) 487–494, https://doi.org/10.1007/s10311-018-0781-0.
[135] N. Li, L. Zhou, X. Jin, G. Owens, Z. Chen, Simultaneous removal of tetracycline and oxytetracycline antibiotics from wastewater using a ZIF-8 metal organic-framework, J. Hazard. Mater. 366 (2019) 563–572, https://doi.org/10.1016/J.JHAZMAT.2018.12.047.
[136] Y. Zhao, X. Gu, S. Gao, J. Geng, X. Wang, Adsorption of tetracycline (TC) onto montmorillonite: cations and humic acid effects, Geoderma 183–184 (2012) 12–18, https://doi.org/10.1016/J.GEODERMA.2012.03.004.
[137] J. Giammarco, V.N. Mochalin, J. Haeckel, Y. Gogotsi, The adsorption of tetracycline and vancomycin onto nanodiamond with controlled release, J. Colloid Interface Sci. 468 (2016) 253–261, https://doi.org/10.1016/J.JCIS.2016.01.062.
[138] P.-H. Chang, Z. Li, T.-L. Yu, S. Munkhbayer, T.-H. Kuo, Y.-C. Hung, J.-S. Jean, K.-H. Lin, Sorptive removal of tetracycline from water by palygorskite, J. Hazard. Mater. 165 (2009) 148–155, https://doi.org/10.1016/J.JHAZMAT.2008.09.113.
[139] M. Shams, E.K. Goharshadi, S. ghaleh Askari, N.T. Nezhad, M. Aziznezhad, Z. D. Nejad, L.D. Wilson, Parameter optimization of tetracycline removal by vanadium oxide nano cuboids, Colloids Surf. A: Physicochem. Eng. Asp. 619 (2021) 126460, https://doi.org/10.1016/j.colsurfa.2021.126460.
[140] Z.W. Zeng, X.F. Tan, Y.G. Liu, S.R. Tian, G.M. Zeng, L.H. Jiang, S.B. Liu, J. Li, N. Liu, Z.H. Yin, Comprehensive adsorption studies of doxycycline and ciprofloxacin antibiotics by biochars prepared at different temperatures, Front. Chem. 6 (2018), https://doi.org/10.3389/fchem.2018.00080.
[141] S. Shi, Y. Fan, Y. Huang, Facile low temperature hydrothermal synthesis of magnetic mesoporous carbon nanocomposite for adsorption removal of ciprofloxacin antibiotics, Ind. Eng. Chem. Res. 52 (2013) 2604–2612, https://doi.org/10.1021/ie303036e.
[142] P. Zhao, F. Yu, R. Wang, Y. Ma, Y. Wu, Sodium alginate/graphene oxide hydrogel beads as permeable reactive barrier material for the remediation of ciprofloxacin-contaminated groundwater, Chemosphere 200 (2018) 612–620, https://doi.org/10.1016/j.chemosphere.2018.02.157.
[143] C.-J.J. Wang, Z. Li, W.-T.T. Jiang, Adsorption of ciprofloxacin on 2:1 dioctahedral clay minerals, Appl. Clay Sci. 53 (2011) 723–728, https://doi.org/10.1016/j.clay.2011.06.014.
[144] C. de Oliveira Carvalho, D.L. Costa Rodrigues, É.C. Lima, C. Santanna Umpierres, D.F. Caicedo Chaguezac, F. Machado Machado, Kinetic, equilibrium, and thermodynamic studies on the adsorption of ciprofloxacin by activated carbon produced from Jerivá (Syagrus romanzoffiana), Environ. Sci. Pollut. Res. 26 (2019) 4690–4702, https://doi.org/10.1007/s11356-018-3954-2.
[145] G. Gopal, M.J. Nirmala, A. Mukherjee, A novel chitosan-coated Fe–Cu CNS loaded with CMC–Alginate composite for adsorptive removal of ciprofloxacin from water, Surf. Interfaces 39 (2023) 102981, https://doi.org/10.1016/j.surfin.2023.102981.
[146] D. Hu, L. Wang, Adsorption of ciprofloxacin from aqueous solutions onto cationic and anionic flax noil cellulose, Desalin. Water Treat. 57 (2016) 28436–28449, https://doi.org/10.1080/19443994.2016.1183232.
[147] S. Wu, X. Zhao, Y. Li, C. Zhao, Q. Du, J. Sun, Y. Wang, X. Peng, Y. Xia, Z. Wang, L. Xia, Adsorption of ciprofloxacin onto biocomposite fibers of graphene oxide/

calcium alginate, Chem. Eng. J. 230 (2013) 389–395, https://doi.org/10.1016/j.cej.2013.06.072.
[148] X. Qin, W. Meng, S. Cheng, B. Xing, C. Shi, Y. Nie, Q. Wang, H. Xia, Efficient removal of heavy metal and antibiotics from wastewater by phosphate-modified hydrochar, Chemosphere 345 (2023) 140484, https://doi.org/10.1016/j.chemosphere.2023.140484.
[149] Y. Sun, J. Zhou, Y. Cheng, J. Yu, W. Cai, Hydrothermal synthesis of modified hydrophobic Zn-Al-layered double hydroxides using structure-directing agents and their enhanced adsorption capacity for p-nitrophenol, Adsorpt. Sci. Technol. 32 (2014) 351–364, https://doi.org/10.1260/0263-6174.32.5.351.
[150] S.E.M. Saber, L.C. Abdullah, T. Ming Ting, S.N.A. Md Jamil, T.S.Y. Choong, G. Abdulkareem-Alsultan, Radiation-induced grafting of glycidyl methacrylate onto natural cotton fibers and trimethylamine modification for p-nitrophenol adsorption, Radiat. Phys. Chem. 209 (2023) 110967, https://doi.org/10.1016/j.radphyschem.2023.110967.
[151] M.J. Ahmed, S.K. Theydan, Adsorptive removal of p-nitrophenol on microporous activated carbon by FeCl3 activation: equilibrium and kinetics studies, Desalin. Water Treat. 55 (2015) 522–531, https://doi.org/10.1080/19443994.2014.920731.
[152] M. Zbair, Z. Anfar, H.A. Ahsaine, Reusable bentonite clay: modelling and optimization of hazardous lead and p-nitrophenol adsorption using a response surface methodology approach, RSC Adv. 9 (2019) 5756–5769, https://doi.org/10.1039/c9ra00079h.
[153] J. Meng, M. Ren, S. Wang, J. Gao, X. Shan, J. Hu, A smart adsorbent with ability of environmentally friendly regeneration for p-nitrophenol removal in aqueous solution, J. Inorg. Organomet. Polym. Mater. 31 (2021) 2381–2392, https://doi.org/10.1007/s10904-020-01792-3.
[154] Z. Jia, M. Jiang, G. Wu, Amino-MIL-53(Al) sandwich-structure membranes for adsorption of p-nitrophenol from aqueous solutions, Chem. Eng. J. 307 (2017) 283–290, https://doi.org/10.1016/j.cej.2016.08.090.
[155] B. Zhang, F. Li, T. Wu, D. Sun, Y. Li, Adsorption of p-nitrophenol from aqueous solutions using nanographite oxide, Colloids Surf. A: Physicochem. Eng. Asp. 464 (2015) 78–88, https://doi.org/10.1016/j.colsurfa.2014.10.020.
[156] A.M. Aldawsari, I.H. Alsohaimi, H.M.A. Hassan, M.R. Berber, Z.E.A. Abdalla, I. Hassan, E.A.M. Saleh, B.H. Hameed, Activated carbon/MOFs composite: AC/NH2-MIL-101(Cr), synthesis and application in high performance adsorption of p-nitrophenol, J. Saudi Chem. Soc. 24 (2020) 693–703, https://doi.org/10.1016/j.jscs.2020.07.009.
[157] M. Ahmaruzzaman, D.K. Sharma, Adsorption of phenols from wastewater, J. Colloid Interface Sci. 287 (2005) 14–24, https://doi.org/10.1016/j.jcis.2005.01.075.
[158] H. Miao, S. Song, H. Chen, W. Zhang, R. Han, G. Yang, Adsorption study of p-nitrophenol on a silver(I) triazolate MOF, J. Porous. Mater. 27 (2020) 1409–1417, https://doi.org/10.1007/s10934-020-00917-w.
[159] S. Giannoulia, I.E. Triantaphyllidou, A.G. Tekerlekopoulou, C.A. Aggelopoulos, Mechanisms of individual and simultaneous adsorption of antibiotics and dyes onto halloysite nanoclay and regeneration of saturated adsorbent via cold plasma bubbling, Nanomaterials 13 (2023) 341, https://doi.org/10.3390/nano13020341.
[160] M.G. Sorkhabi, H. Aghdasinia, F.N. Oskui, A. Karimi, M. Golizadeh, Simultaneous adsorption of chromium and acidic dye from leather tannery model wastewater using a novel modified nanoclay, Environ. Earth Sci. 80 (2021) 813, https://doi.org/10.1007/s12665-021-10120-y.
[161] A. Awasthi, P. Jadhao, K. Kumari, Clay nano-adsorbent: structures, applications and mechanism for water treatment, SN Appl. Sci. 1 (2019) 1–21, https://doi.org/10.1007/s42452-019-0858-9.
[162] P. Stathi, K. Litina, D. Gournis, T.S. Giannopoulos, Y. Deligiannakis, Physicochemical study of novel organoclays as heavy metal ion adsorbents for environmental remediation, J. Colloid Interface Sci. 316 (2007) 298–309, https://doi.org/10.1016/j.jcis.2007.07.078.
[163] T. Chen, Y. Yuan, Y. Zhao, F. Rao, S. Song, Effect of layer charges on exfoliation of montmorillonite in aqueous solutions, Colloids Surf. A: Physicochem. Eng. Asp. 548 (2018) 92–97, https://doi.org/10.1016/j.colsurfa.2018.03.066.
[164] M. Shahbazi, H. Jäger, S.J. Ahmadi, M. Lacroix, Electron beam crosslinking of alginate/nanoclay ink to improve functional properties of 3D printed hydrogel for removing heavy metal ions, Carbohydr. Polym. 240 (2020) 116211, https://doi.org/10.1016/j.carbpol.2020.116211.
[165] S.A. Shaik, J.B. Shaik, A. Goswami, Ethidium bromide adsorption on pyrophyllite nanoclay: insights from batch, thermodynamic, kinetic, and recyclability studies and optimization through response surface methodology, Colloids Surf. A: Physicochem. Eng. Asp. 692 (2024) 133900, https://doi.org/10.1016/j.colsurfa.2024.133900.
[166] L.L. Zhang, A. Zaoui, W. Sekkal, Adsorption efficiency of highly methylene blue dye concentrations with multilayer chitosan-modified clays for a precise nanofiltration performance of polluted water, J. Water Process Eng. 57 (2024) 104651, https://doi.org/10.1016/j.jwpe.2023.104651.
[167] X. Cong, F. Li, R.M. Kelly, N. Xue, Distribution and removal of organochlorine pesticides in waste clay bricks from an abandoned manufacturing plant using low-temperature thermal desorption technology, Environ. Sci. Pollut. Res. 25 (2018) 12119–12126, https://doi.org/10.1007/s11356-018-1422-7.
[168] L.H. Wang, C.I. Lin, Kinetics of heat regeneration of spent bleaching clay, J. Chem. Eng. Japan 33 (2000) 522–525, https://doi.org/10.1252/jcej.33.522.
[169] S.H. Lin, M.J. Cheng, Adsorption of phenol and m-chlorophenol on organobentonites and repeated thermal regeneration, Waste Manag. 22 (2002) 595–603, https://doi.org/10.1016/S0956-053X(01)00029-0.
[170] H. Nourmoradi, M. Nikaeen, H.H. Khiadani, Removal of benzene, toluene, ethylbenzene and xylene (BTEX) from aqueous solutions by montmorillonite modified with nonionic surfactant: equilibrium, kinetic and thermodynamic study, Chem. Eng. J. 191 (2012) 341–348, https://doi.org/10.1016/j.cej.2012.03.029.
[171] J. Zhu, P. Zhang, Y. Wang, K. Wen, X. Su, R. Zhu, H. He, Y. Xi, Effect of acid activation of palygorskite on their toluene adsorption behaviors, Appl. Clay Sci. 159 (2018) 60–67, https://doi.org/10.1016/j.clay.2017.07.019.
[172] Z. Sun, C. Li, D. Wu, Removal of methylene blue from aqueous solution by adsorption onto zeolite synthesized from coal fly ash and its thermal regeneration, J. Chem. Technol. Biotechnol. 85 (2010) 845–850, https://doi.org/10.1002/jctb.2377.
[173] Momina, M. Shahadat, S. Isamil, Regeneration performance of clay-based adsorbents for the removal of industrial dyes: a review, RSC Adv. 8 (2018) 24571–24587, https://doi.org/10.1039/c8ra04290j.
[174] S. Wang, H. Li, S. Xie, S. Liu, L. Xu, Physical and chemical regeneration of zeolitic adsorbents for dye removal in wastewater treatment, Chemosphere 65 (2006) 82–87, https://doi.org/10.1016/j.chemosphere.2006.02.043.
[175] M. Bouraada, M. Lafjah, M.S. Ouali, L.C. de Menorval, Basic dye removal from aqueous solutions by dodecylsulfate- and dodecyl benzene sulfonate-intercalated hydrotalcite, J. Hazard. Mater. 153 (2008) 911–918, https://doi.org/10.1016/j.jhazmat.2007.09.076.
[176] E.I. Unuabonah, A.O. Adedapo, C.O. Nnamdi, A. Adewuyi, M.O. Omorogie, K. O. Adebowale, B.I. Olu-Owolabi, A.E. Ofomaja, A. Taubert, Successful scale-up performance of a novel papaya-clay combo adsorbent: up-flow adsorption of a basic dye, Desalin. Water Treat. 56 (2015) 536–551, https://doi.org/10.1080/19443994.2014.944572.
[177] L. Yang, Z. Zhou, L. Xiao, X. Wang, Chemical and biological regeneration of HDTMA-modified montmorillonite after sorption with phenol, Environ. Sci. Technol. 37 (2003) 5057–5061, https://doi.org/10.1021/es0342493.
[178] R. Zhu, J. Zhu, F. Ge, P. Yuan, Regeneration of spent organoclays after the sorption of organic pollutants: a review, J. Environ. Manag. 90 (2009) 3212–3216, https://doi.org/10.1016/j.jenvman.2009.06.015.
[179] M. Anggraini, A. Kurniawan, L.K. Ong, M.A. Martin, J.C. Liu, F.E. Soetaredjo, N. Indraswati, S. Ismadji, Antibiotic detoxification from synthetic and real effluents using a novel MTAB surfactant-montmorillonite (organoclay) sorbent, RSC Adv. 4 (2014) 16298–16311, https://doi.org/10.1039/c4ra00328d.
[180] A.K. Rahardjo, M.J.J. Susanto, A. Kurniawan, N. Indraswati, S. Ismadji, Modified Ponorogo bentonite for the removal of ampicillin from wastewater, J. Hazard. Mater. 190 (2011) 1001–1008, https://doi.org/10.1016/j.jhazmat.2011.04.052.
[181] M.R.R. Kahkha, M. Kaykhaii, B.R. Kahkha, H. Khosravi, E. Tohidlou, Simultaneous removal of heavy metals from wastewater using modified sodium montmorillonite nanoclay, Anal. Sci. 36 (2020) 1039–1043, https://doi.org/10.2116/analsci.19P300.
[182] R. Antón-Herrero, C. García-Delgado, M. Alonso-Izquierdo, G. García-Rodríguez, J. Cuevas, E. Eymar, Comparative adsorption of tetracyclines on biochars and stevensite: looking for the most effective adsorbent, Appl. Clay Sci. 160 (2018) 162–172, https://doi.org/10.1016/j.clay.2017.12.023.
[183] E.K. Putra, R. Pranowo, J. Sunarso, N. Indraswati, S. Ismadji, Performance of activated carbon and bentonite for adsorption of amoxicillin from wastewater: mechanisms, isotherms and kinetics, Water Res. 43 (2009) 2419–2430, https://doi.org/10.1016/j.watres.2009.02.039.
[184] E. Rivagli, A. Pastorello, M. Sturini, F. Maraschi, A. Speltini, L. Zampori, M. Setti, L. Malavasi, A. Profumo, Clay minerals for adsorption of veterinary FQs: behavior and modeling, J. Environ. Chem. Eng. 2 (2014) 738–744, https://doi.org/10.1016/j.jece.2013.11.017.
[185] S. Das, A. Barui, A. Adak, Montmorillonite impregnated electrospun cellulose acetate nanofiber sorptive membrane for ciprofloxacin removal from wastewater, J. Water Process Eng. 37 (2020) 101497, https://doi.org/10.1016/j.jwpe.2020.101497.
[186] S.K. Sethy, M.V. Kishore, C. Bhagat, M. Kumar, Periodic monitoring of nano clay as the potential adsorbent to remove metal and dyes from wastewater: a review, Total Environ. Res. Themes 7 (2023) 100067, https://doi.org/10.1016/j.totert.2023.100067.
[187] I. Ali, M. Asim, T.A. Khan, Low cost adsorbents for the removal of organic pollutants from wastewater, J. Environ. Manag. 113 (2012) 170–183, https://doi.org/10.1016/j.jenvman.2012.08.028.
[188] S.J. Olusegun, N.D.S. Mohallem, Comparative adsorption mechanism of doxycycline and Congo red using synthesized kaolinite supported CoFe2O4 nanoparticles, Environ. Pollut. 260 (2020) 114019, https://doi.org/10.1016/j.envpol.2020.114019.
[189] J.H. Chi, C.H. Wu, Y.H. Huang, C.M. Shu, Recycling furnace slag and fly ash from industrial byproducts to produce slag/ash based zeolite as a new adsorbent material, Sci. Prog. 104 (2021), https://doi.org/10.1177/00368504221086707.
[190] Y.G. Kang, H. Chi Vu, Y.Y. Chang, Y.S. Chang, Fe(III) adsorption on graphene oxide: a low-cost and simple modification method for persulfate activation, Chem. Eng. J. 387 (2020) 124012, https://doi.org/10.1016/j.cej.2020.124012.
[191] W. Zhang, Y. An, S. Li, Z. Liu, Z. Chen, Y. Ren, S. Wang, X. Zhang, X. Wang, Enhanced heavy metal removal from an aqueous environment using an eco-friendly and sustainable adsorbent, Sci. Rep. 10 (2020) 1–19, https://doi.org/10.1038/s41598-020-73570-7.
[192] R. Foroutan, R. Mohammadi, A.S. Adeleye, S. Farjadfard, Z. Esvandi, H. Arfaeinia, G.A. Sorial, B. Ramavandi, S. Sahebi, Efficient arsenic(V) removal from contaminated water using natural clay and clay composite adsorbents, Environ. Sci. Pollut. Res. 26 (2019) 29748–29762, https://doi.org/10.1007/s11356-019-06070-5.

[193] F. Barraqué, M.L. Montes, M.A. Fernández, R. Candal, R.M. Torres Sánchez, J. L. Marco-Brown, Arsenate removal from aqueous solution by montmorillonite and organo-montmorillonite magnetic materials, Environ. Res. 192 (2021) 110247, https://doi.org/10.1016/j.envres.2020.110247.
[194] R.R. Pawar, Lalhmunsiama, M. Kim, J.-G. Kim, S.-M. Hong, S.Y. Sawant, S.M. Lee, Efficient removal of hazardous lead, cadmium, and arsenic from aqueous environment by iron oxide modified clay-activated carbon composite beads, Appl. Clay Sci. 162 (2018) 339–350, https://doi.org/10.1016/j.clay.2018.06.014.
[195] S. Hokkanen, B. Doshi, V. Srivastava, L. Puro, R. Koivula, Arsenic (III) removal from water by hydroxyapatite-bentonite clay-nanocrystalline cellulose, Environ. Prog. Sustain. Energy 38 (2019) 13147, https://doi.org/10.1002/ep.13147.
[196] S. Mustapha, J.O. Tijani, M.M. Ndamitso, S.A. Abdulkareem, D.T. Shuaib, A. K. Mohammed, A. Sumaila, The role of kaolin and kaolin/ZnO nanoadsorbents in adsorption studies for tannery wastewater treatment, Sci. Rep. 10 (2020) 1–22, https://doi.org/10.1038/s41598-020-69808-z.
[197] K. Moreno-Sader, A. García-Padilla, A. Realpe, M. Acevedo-Morantes, J.B. P. Soares, Removal of heavy metal water pollutants (Co2+ and Ni2+) using polyacrylamide/sodium montmorillonite (PAM/Na-MMT) nanocomposites, ACS Omega 4 (2019) 10834–10844, https://doi.org/10.1021/acsomega.9b00981.
[198] U. Malayoglu, Removal of heavy metals by biopolymer (chitosan)/nanoclay composites, Sep. Sci. Technol. 53 (2018) 2741–2749, https://doi.org/10.1080/01496395.2018.1471506.
[199] K.D. Nguyen, T.T.C. Trang, T. Kobayashi, Chitin-halloysite nanoclay hydrogel composite adsorbent to aqueous heavy metal ions, J. Appl. Polym. Sci. 136 (2019) 47207, https://doi.org/10.1002/app.47207.
[200] S. Elhami, S. Shafizadeh, Removal of mercury (II) using modified nanoclay, Mater. Today Proc. 3 (2016) 2623–2627, https://doi.org/10.1016/j.matpr.2016.06.005.
[201] L. Li, J. Iqbal, Y. Zhu, P. Zhang, W. Chen, A. Bhatnagar, Y. Du, Chitosan/Ag-hydroxyapatite nanocomposite beads as a potential adsorbent for the efficient removal of toxic aquatic pollutants, Int. J. Biol. Macromol. 120 (2018) 1752–1759, https://doi.org/10.1016/j.ijbiomac.2018.09.190.
[202] K. Kalantari, M.B. Ahmad, H.R. Fard Masoumi, K. Shameli, M. Basri, R. Khandanlou, Rapid and high capacity adsorption of heavy metals by Fe3O4/montmorillonite nanocomposite using response surface methodology: preparation, characterization, optimization, equilibrium isotherms, and adsorption kinetics study, J. Taiwan Inst. Chem. Eng. 49 (2015) 192–198, https://doi.org/10.1016/j.jtice.2014.10.025.
[203] Y.-M. Chen, T.-M. Tsao, M. Wang, S. Yu, C.-C. Liu, H.-C. Li, C.-Y. Chiu, L.-C. Wang, Kinetic and thermodynamic studies on removal of Cu(II) from aqueous solutions using soil nanoclays, Water Environ. Res. 87 (2015) 88–95, https://doi.org/10.2175/106143014x14062131179159.
[204] J. Kyzioł-Komosińska, J. Janeczek, T. Krzykawski, M.J. Fabiańska, A. Matuszewska, A. Dzieniszewska, E. Teper, M. Pająk, N. Sawicka, Adsorption of Eu(III) onto bentonite and phyllite: a comparative study, Appl. Clay Sci. 183 (2019) 105330, https://doi.org/10.1016/j.clay.2019.105330.
[205] W.R. Lim, C.H. Lee, C.M. Lee, The removal of strontium ions from an aqueous solution using Na-A zeolites synthesized from kaolin, Materials (Basel) 17 (2024) 575, https://doi.org/10.3390/ma17030575.
[206] A.Q. Alorabi, M.S. Hassan, M.M. Alam, S.A. Zabin, N.I. Alsenani, N.E. Baghdadi, Natural clay as a low-cost adsorbent for crystal violet dye removal and antimicrobial activity, Nanomaterials 11 (2021) 2789, https://doi.org/10.3390/nano11112789.
[207] R. El Haouti, H. Ouachtak, A. El Guerdaoui, A. Amedlous, E. Amaterz, R. Haounati, A.A. Addi, F. Akbal, N. El Alem, M.L. Taha, Cationic dyes adsorption by Na-montmorillonite nano clay: experimental study combined with a theoretical investigation using DFT-based descriptors and molecular dynamics simulations, J. Mol. Liq. 290 (2019) 111139, https://doi.org/10.1016/j.molliq.2019.111139.
[208] M.V. Nagarpita, P. Roy, S.B. Shruthi, R.R.N. Sailaja, Synthesis and swelling characteristics of chitosan and CMC grafted sodium acrylate-co-acrylamide using modified nanoclay and examining its efficacy for removal of dyes, Int. J. Biol. Macromol. 102 (2017) 1226–1240, https://doi.org/10.1016/j.ijbiomac.2017.04.099.
[209] H. Kaşgöz, A. Durmus, Dye removal by a novel hydrogel-clay nanocomposite with enhanced swelling properties, Polym. Adv. Technol. 19 (2008) 838–845, https://doi.org/10.1002/pat.1045.
[210] D.S. Tong, C.W. Wu, M.O. Adebajo, G.C. Jin, W.H. Yu, S.F. Ji, C.H. Zhou, Adsorption of methylene blue from aqueous solution onto porous cellulose-derived carbon/montmorillonite nanocomposites, Appl. Clay Sci. 161 (2018) 256–264, https://doi.org/10.1016/j.clay.2018.02.017.
[211] S. Radoor, J. Karayil, J. Parameswaranpillai, S. Siengchin, Adsorption of methylene blue dye from aqueous solution by a novel PVA/CMC/halloysite nanoclay bio composite: characterization, kinetics, isotherm and antibacterial properties, J. Environ. Health Sci. Eng. 18 (2020) 1311–1327, https://doi.org/10.1007/s40201-020-00549-x.
[212] A. Maged, O.E.A. Al-Hagar, S. Ahmed Abu El-Magd, S. Kharbish, A. Bhatnagar, D. Abol-Fotouh, O.E.A. Al-Hagar, S. Ahmed Abu El-Magd, S. Kharbish, A. Bhatnagar, D. Abol-Fotouh, Bacterial nanocellulose-clay film as an eco-friendly sorbent for superior pollutants removal from aqueous solutions, Environ. Res. 257 (2024) 119231, https://doi.org/10.1016/j.envres.2024.119231.
[213] V. Arya, L. Philip, Adsorption of pharmaceuticals in water using Fe 3 O 4 coated polymer clay composite, Microporous Mesoporous Mater. 232 (2016) 273–280, https://doi.org/10.1016/j.micromeso.2016.06.033.
[214] Y. Hu, C. Pan, X. Zheng, S. Liu, F. Hu, L. Xu, G. Xu, X. Peng, Removal of ciprofloxacin with aluminum-pillared kaolin sodium alginate beads (CA-Al-KABs): kinetics, isotherms, and BBD model, Water (Switzerland) 12 (2020) 905, https://doi.org/10.3390/w12030905.
[215] A. Maged, A.M. Elgarahy, N.H. Haneklaus, A.K. Gupta, P.-L. Show, A. Bhatnagar, Sustainable functionalized smectitic clay-based nano hydrated zirconium oxides for enhanced levofloxacin sorption from aqueous medium, J. Hazard. Mater. 452 (2023) 131325, https://doi.org/10.1016/J.JHAZMAT.2023.131325.
[216] L. Rafati, M.H. Ehrampoush, A.A. Rafati, M. Mokhtari, A.H. Mahvi, Removal of ibuprofen from aqueous solution by functionalized strong nano-clay composite adsorbent: kinetic and equilibrium isotherm studies, Int. J. Environ. Sci. Technol. 15 (2018) 513–524, https://doi.org/10.1007/s13762-017-1393-0.
[217] W.S. Wan Ngah, N.F.M. Ariff, M.A.K.M. Hanafiah, Preparation, characterization, and environmental application of crosslinked chitosan-coated bentonite for tartrazine adsorption from aqueous solutions, Water Air Soil Pollut. 206 (2010) 225–236, https://doi.org/10.1007/s11270-009-0098-5.
[218] L. Ma, Q. Chen, J. Zhu, Y. Xi, H. He, R. Zhu, Q. Tao, G.A. Ayoko, Adsorption of phenol and Cu(II) onto cationic and zwitterionic surfactant modified montmorillonite in single and binary systems, Chem. Eng. J. 283 (2016) 880–888, https://doi.org/10.1016/j.cej.2015.08.009.
[219] A. Gładysz-Płaska, M. Majdan, S. Pikus, D. Sternik, Simultaneous adsorption of chromium(VI) and phenol on natural red clay modified by HDTMA, Chem. Eng. J. 179 (2012) 140–150, https://doi.org/10.1016/j.cej.2011.10.071.
[220] H. Fan, L. Zhou, X. Jiang, Q. Huang, W. Lang, Adsorption of Cu2+ and methylene blue on dodecyl sulfobetaine surfactant-modified montmorillonite, Appl. Clay Sci. 95 (2014) 150–158, https://doi.org/10.1016/j.clay.2014.04.001.
[221] G. Wang, S. Zhang, Y. Hua, X. Su, S. Ma, J. Wang, Q. Tao, Y. Wang, S. Komarneni, Phenol and/or Zn2 + adsorption by single- or dual-cation organomontmorillonites, Appl. Clay Sci. 140 (2017) 1–9, https://doi.org/10.1016/j.clay.2017.01.023.
[222] C. Liu, P. Wu, Y. Zhu, L. Tran, Simultaneous adsorption of Cd2+ and BPA on amphoteric surfactant activated montmorillonite, Chemosphere 144 (2016) 1026–1032, https://doi.org/10.1016/j.chemosphere.2015.09.063.